

# Latest Trends on the Future of Three-Dimensional Separations in Chromatography

Noor Abdulhussain,\* Suhas Nawada, and Peter Schoenmakers

Cite This: *Chem. Rev.* 2021, 121, 12016–12034

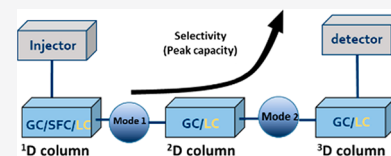
Read Online

ACCESS |

Metrics &amp; More

Article Recommendations

**ABSTRACT:** Separation and characterization of complex mixtures are of crucial importance in many fields, where extremely high separation power is required. Three-dimensional separation techniques can offer a path toward achieving high peak capacities. In this Review, online three-dimensional separation systems are discussed, including three-dimensional gas chromatography, and hyphenated combinations of two-dimensional gas chromatography with liquid chromatography or supercritical-fluid chromatography. Online comprehensive two-dimensional liquid chromatography provides detailed information on complex samples and the need for higher peak capacities is pushing researchers toward online three-dimensional liquid chromatography. In this review, an overview of the various combinations are provided and we discuss and compare their potential performance, advantages, perspectives, and results obtained during the most recent 10–15 years. Finally, the Review will discuss a novel approach of spatial three-dimensional liquid separation to increase peak capacity.



## CONTENTS

|   |       |
|---|-------|
| 1. Introduction                                     | 12016 |
| 2. Multidimensional-GC                              | 12018 |
| 2.1. Instrumentation Design                         | 12018 |
| 2.1.1. Physical Considerations                      | 12021 |
| 2.2. Column Considerations                          | 12021 |
| 2.3. Peak Capacity                                  | 12022 |
| 2.3.1. Data-Analysis Algorithms                     | 12022 |
| 2.4. Coupling to Various Chromatographic Approaches | 12023 |
| 3. Three-Dimensional-Liquid Chromatography          | 12026 |
| 4. Spatial 3D Separation                            | 12030 |
| 5. Conclusions                                      | 12031 |
| Author Information                                  | 12031 |
| Corresponding Author                                | 12031 |
| Authors   | 12031 |
| Notes   | 12031 |
| Biographies   | 12031 |
| Acknowledgments                                     | 12032 |
| References  | 12032 |

## 1. INTRODUCTION

Multidimensional separation methods are very attractive and widely used in the separation of complex samples. The past decades have seen the frontiers of analytical sciences expand to the analysis of increasingly complex samples, with system setups capable of reaching ever-increasing peak capacities. According to Davis and Giddings, the concept of peak capacity provides a means for calculating the maximum number of resolvable components in a chromatographic run.<sup>1</sup> However,

the number of components that are likely to be resolved in a chromatogram is only a fraction of the total peak capacity. Therefore, extremely high values of the peak capacity are required for the separation of complex samples. Ideally, the peak capacity of a multidimensional separation system is simply the product of the peak capacities of each dimension. In practice, several factors during multidimensional separation (listed in Table 1), such as undersampling of the first-dimension effluent and injection band broadening in the second dimension are minimized,<sup>2</sup> which can undermine the final peak capacity (see Table 1).

Besides achieving peak capacity, other factors, such as orthogonality, detectability and analysis time, also play a role in achieving adequate conditions to separate complex mixtures. Sample complexity is not only related to the number of components in a sample, but also to the number and range of different chemical classes. Consequently, the analysis of complex mixtures would require high selectivity, high sensitivity, a wide dynamic range, and high separation power.

In liquid chromatography (LC), the researcher is confronted with a trade-off between the peak capacity and the analysis time.<sup>5</sup> When using one-dimensional LC, high peak capacities (of 1000 or more) are achievable only at the expense of very long analysis times. A way to overcome this problem is to use

**Special Issue:** Frontiers of Analytical Science

**Received:** November 24, 2020

**Published:** April 20, 2021



**Table 1. Critical Factors Influencing the Actual, Effective Peak Capacity in Comprehensive Two-Dimensional Chromatography**

|   | GC × GC  | LC × LC  |
|---|--|--|
| undersampling of the first-dimension separation | four cuts per peak may be approached by very fast 2D separations   | undersampling is the norm, with 2 or 3 cuts per peak thought optimal from a time perspective <sup>2,3</sup><br>many LC × LC applications involve fewer 2D runs and massive undersampling                 |
| second-dimension injection effect               | effects can be minimized by effective modulation methods   | passive modulation causes large 2D injection volumes, which may be compensated by high 2D flow rates (requiring large amounts of solvent) <sup>2,4</sup><br>active modulation may alleviate these issues |
| suboptimal conditions                           | usually, the mass flow of carrier gas is the same in both dimensions, causing suboptimal conditions in either or both  | 1D effluent may be a poor 2D injection solvent<br>active modulation may mitigate such effects  |
| orthogonality                                   | limited orthogonality leaves a part of the separation space unoccupied and part of the theoretical peak capacity unused<br>orthogonality may be enhanced by choosing different stationary phases | many different retention mechanisms may be applied for different samples   |

comprehensive multidimensional chromatography. To efficiently make use of the increased resolving power in multidimensional chromatography, the retention mechanism for each dimension must be sufficiently different. We, then, speak of an “orthogonal” separation if the retention times in the two dimensions are independent. This could aid with analyzing the increasingly complex samples. In online comprehensive two-dimensional chromatography, the first dimension effluent is divided in a large number of fractions, ideally such that the first-dimension separation remains intact, with the resolution obtained in the first dimension being maintained upon modulation to the second dimension. All these fractions are then subsequently and in real-time separated on a fast second-dimension system. If only one fraction is singled out for separation in the second dimension we speak of heart-cut 2D-LC. If a small number of fractions is subjected to a second-dimension separation, we speak of multiple heart-cut 2D-LC or selective-comprehensive 2D-LC.<sup>6</sup>

Online comprehensive two-dimensional liquid chromatography (LC × LC) has become an attractive method to provide information on sample components and sample classes taking into account the sample dimensionality<sup>7</sup> by using various chromatographic modes. It is now commonly used for the analysis of complex samples, such as in proteomics studies, polymer science or petroleum analysis. There are some challenges within the LC × LC system, which is that LC × LC separations might take longer than 1D-LC separations and undersampling problems may occur. Analytes can be resolved by 1D separation can be mixed back together if the fractions collected are larger in volume (or time) than the volume of the peaks as they elute the 1D column. Undersampling results in loss of 1D resolution and quantitative and qualitative information. Several reviews explore the current state of the art and challenges in two-dimensional LC (2D-LC).<sup>8–11</sup> Although 2D-LC, and especially LC × LC methods have proven powerful, the potential of further gain in peak capacities has pushed researchers to explore three-dimensional (3D) separations. In conventional time-based gradient-elution 1D-LC, the peak capacity ( ${}^1n_c$ ) can be approximated by eq 1, which can be rewritten as

$${}^1n_c \approx \frac{t_G}{t_0} \frac{\sqrt{L}}{4 \cdot R_s \cdot (1 + k_c) \cdot \sqrt{H}} + 1 \quad (1)$$

where  $t_G$  is the duration of the gradient,  $t_0$  the column hold-up time,  $R_s$  is the desired resolution,  $k_c$  the retention factor at the moment of the elution,  $L$  the column length, and  $H$  the

(average) plate height. In a time-based 3D-LC system, the total peak capacity ( ${}^3n_c$ ) can be approximated as the product of the peak capacities of each dimension. The implementation of a comprehensive 3D chromatographic system is extremely challenging and such separations have yet to be proven as a method accepted by the industry. Guiochon et al. studied the possibilities of coupling three separations in terms of practical application, anticipated performance, and technical challenges.<sup>11</sup> So far, 3D-online liquid-phase separations have rarely been reported. The first such separation was performed by Moore and Jorgenson who applied it for the separation of peptide digests.<sup>12</sup> This was achieved by coupling a slow (5 h) size exclusion chromatography (SEC) separation as the first dimension, with a faster (6 min) separation by reversed-phase liquid chromatography (RPLC) in the second dimension, and a very fast (2 s) separation by capillary electrophoresis (CE) in the third dimension. Although this three-dimensional liquid-phase separation system is impressive, the analysis time and the extreme demands on the speed and robustness of the third-dimension separation proved to be prohibitive. Over the years the technology for coupling the different separation stages, known as modulation has improved, allowing renewed attempts to realize comprehensive 3D-LC systems mostly for separation of peptides in the field of proteomics. The realization of heart-cut 3D-LC systems is much less challenging and such systems have found applications in, for example, the purification of biopharmaceuticals for analytical or preparative purposes. This Review will cover recent developments in comprehensive 3D-LC systems.

Comprehensive two-dimensional gas chromatography (GC × GC) has become an established technique in many domains, such as the food industry<sup>13,14</sup> and petroleum industries.<sup>15</sup> GC × GC provides more separation power than one-dimensional (1D)-GC, increased sensitivity, and chemical selectivity by the addition of the second dimension. GC × GC benefits greatly from the large peak capacity compared to 1D-GC. The peak capacity,  ${}^1n_c$ , in a 1D separation at the resolution,  $R_s = 1$  can be approximated as the separation time,  ${}^1t$ , divided by the average width-of-base ( $4\sigma$ ),  ${}^1W$ .

$${}^1n_c = \frac{{}^1t}{{}^1W} \quad (2)$$

The ideal peak capacity for GC × GC can be approximated by the product of the peak capacities of the individual dimensions.

$$n_{c,2D} = {}^1n_c \times {}^2n_c = \frac{{}^1t}{{}^1W} \frac{{}^2t}{{}^2W} = \frac{{}^1t}{{}^1W} \frac{{}^{12}t_{\text{mod}}}{{}^2W} \quad (3)$$

Here,  ${}^{12}t_{\text{mod}}$  is the time per modulation (or modulation period) from the first ( ${}^1D$ ) to the second ( ${}^2D$ ) dimension, which equals the second-dimension analysis time ( ${}^2t$ ). The same approach can be applied for the addition of a third separation dimension. The ideal peak capacity for comprehensive 3D-GC (GC  $\times$  GC  $\times$  GC) can be approximated as

$$n_{c,3D} = {}^1n_c \times {}^2n_c \times {}^3n_c = \frac{{}^1t}{{}^1W} \frac{{}^2t}{{}^2W} \frac{{}^3t}{{}^3W} = \frac{{}^1t}{{}^1W} \frac{{}^{12}t_{\text{mod}}}{{}^2W} \frac{{}^{23}t_{\text{mod}}}{{}^3W} \quad (4)$$

where  ${}^{23}t_{\text{mod}}$  is the modulation period for coupling the  ${}^2D$  and  ${}^3D$  separations. The average peak width at the base ( $4\sigma$ ) for each dimension is given by  ${}^1W$ ,  ${}^2W$ , and  ${}^3W$ , respectively. In terms of modulation periods instead of separation run times of 2D and 3D, eq 4 can be obtained. If a mixture features clear and dominant sample dimensions, as is the case in mineral oils, structured chromatograms can be obtained that facilitate qualitative analysis. A third GC dimension may be added to create comprehensive three-dimensional gas chromatography,<sup>16–20</sup> but the chemical selectivity may be enhanced further by adding different dimensions. For example, the online coupling of LC,<sup>21–24</sup> or supercritical fluid chromatography (SFC)<sup>25–27</sup> to GC  $\times$  GC may enhance so-called “group-type” separations of different classes of compounds.

Mass spectrometry (MS) is arguably also a separation method. If soft-ionization methods are employed, such as chemical ionization in combination with GC or electrospray ionization (ESI) in combination with LC, MS yields a separation based on analyte molar mass (or, more precisely, based on the mass-to-charge ratio), as well as valuable qualitative molecular-weight information or molecular-formula information when using HRMS. When using more harsh ionization techniques, such as electron ionization in combination with GC or when tandem-MS techniques are used, attention shifts toward more qualitative information. In most cases, it is highly advisable to use MS in combination with multidimensional liquid-phase or gas-phase separations because much more information can be obtained within the same analysis time. An exception is the use of GC  $\times$  GC for group-type separations and class-based quantitation.

In recent years, ion-mobility spectrometry has emerged as an additional method to obtain separation of and quantitative information on the analytes. The fundamental difference is that, whereas MS ions move in a vacuum, in IMS they move into a counter flow of inert gas (typically helium). In combination with MS, IMS yields additional and different selectivity, creating possibilities to separate isomers. As an interim step in GC-IMS-MS or LC-IMS-MS IMS offers little additional selectivity. IMS-MS is very much faster than GC-MS or LC-MS, but much more likely to suffer from serious matrix effects. While there is something to be said for treating MS and IMS as separation techniques, it is not common to refer to the ubiquitous LC-MS techniques as two-dimensional separations. Therefore, we feel it is inconsistent to refer to, for example, GC  $\times$  GC-MS, LC  $\times$  LC-MS, or LC-IMS-MS as three-dimensional separations.

As a consequence, we will focus in this review on chromatographic separations. We aim to cover the state of the art in 3D-separation with various combinations of GC, LC, or SFC, as well as liquid-phase spatial separations. We will

cover online GC  $\times$  GC  $\times$  GC, LC  $\times$  LC  $\times$  LC, and SFC  $\times$  GC  $\times$  GC techniques. Regarding LC-GC  $\times$  GC techniques, we are discussing off-line technique because of the limited online techniques available in the literature. We will discuss and compare the potential performance of these combinations, their advantages and limitations, results obtained, and future perspectives. The Review will then progress to discuss a novel approach of spatial separation aimed at increasing peak capacity. This Review is largely limited to online 3D separation systems and as such does not cover off-line methods. These have already been extensively discussed elsewhere.<sup>28</sup>

## 2. MULTIDIMENSIONAL-GC

Comprehensive two-dimensional (2D) gas chromatography (GC  $\times$  GC) was conceptually described by Giddings<sup>29</sup> and experimentally realized by Liu and Philips.<sup>30</sup> The modern GC  $\times$  GC platform provides highly effective methods for the separation of complex volatile samples. In addition, GC  $\times$  GC provides a much-enhanced chemical selectivity through the use of the second-dimension separation, which results in better (group-type) separation. Typical peak capacities of 1D-GC separations are of the order of 1000, whereas GC  $\times$  GC may readily provide peak capacities in excess of 20 000. Multiple reviews on GC  $\times$  GC have been published recently covering many aspects of the field from application and instrumentation to data analysis.<sup>31,32</sup> To further enhance chemical selectivity, it is intriguing to consider higher-order instruments, specifically to provide comprehensive three-dimensional (GC  $\times$  GC  $\times$  GC) separations. Notable literature has been summarized in Table 2, which lists all the online 3D-GC platforms published to our knowledge so far. The applications are grouped into several categories based on the type of sample. Comprehensive couplings of two dimensions are denoted with “ $\times$ ”, while heart-cutting methods are denoted with “–”. Further, we classified through the type of modulation used between 1D and 2D (mode 1) and between 2D and 3D (mode 2). Within each dimension, the type of retention mechanism, stationary phase, and the dimension of the column are included. The modulation types are abbreviated as follows, three/six-port valves (PV), thermal modulation (TM), (high-temperature)-diaphragm valves ((HT)-DV), cryogenic trapping (CT), Dean switch (DS), pulse flow valve (PFV), thermal desorption (TD), and differential flow modulator (DF). Also, for each application, the reported peak capacity is listed, which will be discussed further in this review.

### 2.1. Instrumentation Design

The GC  $\times$  GC  $\times$  GC experiment requires three separation columns connected online through two modulators, ideally assembled with a minimal complication of hardware. It should be able to produce chromatographic bandwidths narrow enough to generate large data sets in reasonable analysis times, and it requires robust and user-friendly software for visualizing and interpreting GC data.<sup>33</sup> To realize GC  $\times$  GC and GC  $\times$  GC  $\times$  GC, it is crucial that the subsequent dimension is much faster than the previous one. If the next dimension is 100 times faster, the initial chromatogram can be divided in 100 fractions. In GC  $\times$  GC  $\times$  GC, the third dimension should then be 10 000 times faster than the first dimension. The best way to drastically influence the speed of analysis in open-tubular (capillary) GC is by changing the column diameter. However, the optimal volumetric flow rate scales roughly with the column diameter (the two are

Table 2. Overview of Three-Dimensional Gas Chromatography Separation Systems<sup>a</sup>

| application   | 1D (type, dimensions $L$ (m) $\times$ i.d. ( $\mu\text{m}$ ), film thickness, $d_f$ ( $\mu\text{m}$ ))                 | mode 1  | 2D (type, dimensions $L$ (m) $\times$ i.d. ( $\mu\text{m}$ ), film thickness, $d_f$ ( $\mu\text{m}$ ))   | mode 2 | 3D (type, dimensions $L$ (m) $\times$ i.d. ( $\mu\text{m}$ ), film thickness, $d_f$ ( $\mu\text{m}$ ))   | detection      | peak capacity | remarks  | ref |
|---|--|---------|--|--------|--|----------------|---------------|--|-----|
| mixture of dodecane, tridecane, and tetra-decane      | nonpolar (dimethylpolysiloxane, 0.2 m $\times$ 100 $\mu\text{m}$ i.d., $d_f$ 3.5 $\mu\text{m}$ )                       | TM      | medium-polar (14% cyanopropyl-phenyl-methyl polysiloxane, 3 m $\times$ 100 $\mu\text{m}$ i.d., $d_f$ 0.2 $\mu\text{m}$ )   | TM     | medium-polar (50% phenyl-polysiloxane, 0.5 m $\times$ 100 $\mu\text{m}$ i.d., $d_f$ 0.1 $\mu\text{m}$ )  | FID            | –             | first 3D-GC system developed   | 33  |
| mixture of hydrocarbons                               | nonpolar (5% phenyl-methyl polysiloxane, 25 m $\times$ 530 $\mu\text{m}$ i.d., $d_f$ 5 $\mu\text{m}$ )                 | DV      | medium-polar (trifluoropropyl-methyl polysiloxane, 5 m $\times$ 250 $\mu\text{m}$ i.d., $d_f$ 1 $\mu\text{m}$ )  | DV     | polar (poly(ethylene glycol), 0.55 m/1 m $\times$ 100 $\mu\text{m}$ i.d., $d_f$ 0.1 $\mu\text{m}$ )  | FID            | 3500          | usage of PARAFAC algorithm   | 17  |
| diesel sample   | nonpolar (5% phenyl-methyl polysiloxane, 30 m $\times$ 250 $\mu\text{m}$ i.d., $d_f$ 5 $\mu\text{m}$ )                 | DV      | highly polar (1,9-di(3-vinyl imidazolium) nonane bis [(trifluoromethyl) sulfonyl] imidate, 4 m $\times$ 100 $\mu\text{m}$ i.d., $d_f$ 0.08 $\mu\text{m}$ )       | DV     | polar (poly(ethylene glycol), 1 m $\times$ 100 $\mu\text{m}$ i.d., $d_f$ 0.1 $\mu\text{m}$ )   | FID            | –             | –  | 18  |
| volatile organic compounds (VOCs)                     | medium-polar (5% diphenyl, 95% dimethylpolysiloxane, 0.8 m $\times$ 250 $\mu\text{m}$ i.d.)                            | PV      | nonpolar (dimethyl polysiloxane, 1 m $\times$ 250 $\mu\text{m}$ i.d.)  | PV     | polar (dimethyl polysiloxane, 1 m $\times$ 250 $\mu\text{m}$ i.d.)   | vapor detector | –             | –  | 34  |
| 115-component test mixture and spiked diesel          | medium-polar (5% phenyl-methyl polysiloxane, 30 m $\times$ 250 $\mu\text{m}$ i.d., $d_f$ 0.50 $\mu\text{m}$ )          | (HT)-DV | polar (poly(ethylene glycol), 3.5 m $\times$ 180 $\mu\text{m}$ i.d., $d_f$ 0.18 $\mu\text{m}$ )  | TM     | medium-polar (trifluoropropyl-methyl polysiloxane, 1 m $\times$ 100 $\mu\text{m}$ i.d., $d_f$ 0.1 $\mu\text{m}$ )                                    | ToF-MS         | 5000–9600     | –  | 35  |
| 115-component test mixture and spiked diesel          | medium-polar (5% phenyl-methyl polysiloxane, 30 m $\times$ 250 $\mu\text{m}$ i.d., $d_f$ 0.50 $\mu\text{m}$ )          | (HT)-DV | polar (poly(ethylene glycol), 3.5 m $\times$ 180 $\mu\text{m}$ i.d., $d_f$ 0.18 $\mu\text{m}$ )  | TM     | medium-polar (trifluoropropyl-methyl polysiloxane, 1 m $\times$ 100 $\mu\text{m}$ i.d., $d_f$ 0.1 $\mu\text{m}$ )                                    | ToF-MS         | –             | improvement on PARAFAC algorithm   | 19  |
| E and Z isomers of oximes                             | chiral (diethyl-terbutylsilyl- $\beta$ -cyclodextrin, 25 m $\times$ 250 $\mu\text{m}$ i.d., $d_f$ 0.25 $\mu\text{m}$ ) | CT      | highly polar (1,5-di (2,3-dimethyl imidazolium) pentanebis (trifluoro-methane sulfonyl) imide, 1.8 m $\times$ 100 $\mu\text{m}$ i.d., $d_f$ 0.10 $\mu\text{m}$ ) | DS     | nonpolar ((5% phenyl)-methyl polysiloxane, 30 m $\times$ 250 $\mu\text{m}$ i.d., $d_f$ 0.25 $\mu\text{m}$ )  | QToF-MS        | –             | –  | 36  |
| 115-component test mixture and spiked diesel          | medium-polar (50% phenyl/50% methylpolysiloxane, 20 m $\times$ 180 $\mu\text{m}$ i.d., $d_f$ 0.18 $\mu\text{m}$ )      | (HT)-DV | nonpolar (poly(5% diphenyl/95% dimethyl siloxane, 6 m $\times$ 100 $\mu\text{m}$ i.d., $d_f$ 0.10 $\mu\text{m}$ )  | PV     | highly polar (poly(ethylene glycol), 1 m $\times$ 100 $\mu\text{m}$ i.d., $d_f$ 0.10 $\mu\text{m}$ )   | FID            | ~10000        | total analysis time of 11 min was achieved                                     | 20  |
| 115-component test mixture                            | medium-polar (5% phenyl/95% dimethylpolysiloxane, 40 m $\times$ 180 $\mu\text{m}$ i.d., $d_f$ 0.40 $\mu\text{m}$ )     | (HT)-DV | nonpolar (50% phenyl/50% dimethylpolysiloxane, 3 m $\times$ 100 $\mu\text{m}$ i.d., $d_f$ 0.10 $\mu\text{m}$ )   | PV     | highly polar (poly(ethylene glycol), 0.5 m $\times$ 100 $\mu\text{m}$ i.d., $d_f$ 0.10 $\mu\text{m}$ )   | FID            | 30600         | optimization of the 3D-GC system by manipulation the ratio of the phase volume | 37  |
| mixture of hydrocarbons                               | nonpolar (5% phenyl-methyl polysiloxane, 40 m $\times$ 180 $\mu\text{m}$ i.d., $d_f$ 0.18 $\mu\text{m}$ )              | TM      | medium-polar (trifluoropropylmethyl polysiloxane, 2.5 m $\times$ 180 $\mu\text{m}$ i.d., $d_f$ 0.18 $\mu\text{m}$ )  | PV     | polar (poly(ethylene glycol), 1.0 m $\times$ 180 $\mu\text{m}$ i.d., $d_f$ 0.18 $\mu\text{m}$ )  | TOF-MS         | 35000         | pulse flow valve modulation was performed in a negative mode                   | 16  |
| algae-derived fuel oils                               | polar (poly(ethylene glycol in sol-gel matrix, 30 m $\times$ 320 $\mu\text{m}$ i.d., $d_f$ 0.5 $\mu\text{m}$ )         | CT      | medium-polar (5% phenylmethyl polysiloxane, 5 m $\times$ 150 $\mu\text{m}$ i.d., $d_f$ 0.15 $\mu\text{m}$ )  | DS     | medium-polar (50% phenyl/50% dimethyl polysiloxane, 20 m $\times$ 180 $\mu\text{m}$ i.d., $d_f$ 0.18 $\mu\text{m}$ )                                 | FID            | 3600          | –  | 38  |
| essential oil ( <i>Clausena lansium</i> Skeels plant) | nonpolar (poly(5% diphenyl/95% dimethylsiloxane), 30 m $\times$ 530 $\mu\text{m}$ i.d., $d_f$ 5.0 $\mu\text{m}$ )      | DS      | polar (poly(ethylene glycol 30 m $\times$ 530 $\mu\text{m}$ i.d., $d_f$ 2.0 $\mu\text{m}$ )  | DS     | polar (1,12-di (tripropyl phosphonium) dodecane bis(trifluoromethanesulfone) imide, 30 m $\times$ 530 $\mu\text{m}$ i.d., $d_f$ 0.85 $\mu\text{m}$ ) | 3 FIDs         | –             | three GC-instruments coupled together  | 39  |
| essential oils (Agarwood)                             | nonpolar ((5%-phenyl)-methyl polysiloxane,   | CT      | polar (poly(ethylene glycol 30 m $\times$ 250 $\mu\text{m}$ i.d., $d_f$ 0.25 $\mu\text{m}$ )   | DS     | polar (1,12-di (tripropyl phosphonium) dodecane bis(trifluoromethanesulfone) imide, 30 m $\times$ 250 $\mu\text{m}$ i.d., $d_f$ 0.85 $\mu\text{m}$ ) | QToF-MS        | 5000          | –  | 40  |



Table 2. continued

| application | 1D (type, dimensions $L$ (m) $\times$ i.d. ( $\mu\text{m}$ ), film thickness, $d_f$ ( $\mu\text{m}$ ))   | mode 1             | 2D (type, dimensions $L$ (m) $\times$ i.d. ( $\mu\text{m}$ ), film thickness, $d_f$ ( $\mu\text{m}$ ))  | mode 2             | 3D (type, dimensions $L$ (m) $\times$ i.d. ( $\mu\text{m}$ ), film thickness, $d_f$ ( $\mu\text{m}$ ))   | detection | peak capacity | remarks           | ref |
|-------------|--|--------------------|---|--------------------|--|-----------|---------------|-------------------|-----|
| allergens   | <p>30 m <math>\times</math> 250 <math>\mu\text{m}</math> i.d., <math>d_f</math> 0.25 <math>\mu\text{m}</math>)</p> <p>nonpolar ((5%-phenyl)-methyl polysiloxane, 30 m <math>\times</math> 250 <math>\mu\text{m}</math> i.d., <math>d_f</math> 0.25 <math>\mu\text{m}</math>)</p> | <p>×</p> <p>TD</p> | <p>natural products</p> <p>polar (1,12-Di (tripropyl-phosphonium) dodecane bis(trifluoromethanesulfonyl) imide trifluoro-methanesulfonate, 1 m <math>\times</math> 100 <math>\mu\text{m}</math> i.d., <math>d_f</math> 0.08 <math>\mu\text{m}</math>)</p> | <p>×</p> <p>DF</p> | <p>thanesulfonyl) imide, 1.4 m <math>\times</math> 100 <math>\mu\text{m}</math> i.d., <math>d_f</math> 0.08 <math>\mu\text{m}</math>)</p> <p>highly polar (polyethylene glycol, 3.0 m <math>\times</math> 200 <math>\mu\text{m}</math> i.d., <math>d_f</math> 0.10 <math>\mu\text{m}</math>)</p> | FID       | 9821          | PARAFAC algorithm | 16  |

<sup>a</sup>The couplings are  $\times$  = comprehensive,  $-$  = heart-cut. The modulation types are PV = 3/6-port valves, TM = thermal modulation, (HT)-DV = (high-temperature)-diaphragm valves, CT = cryogenic trapping, DS = dean switch, PFV = pulse-flow valve, TD = thermal desorption modulator, DF = differential-flow modulator, FID = flame-ionization detector, QTOF-MS = quadrupole-time-of-flight mass spectrometer.

proportional if gas compression is neglected). In GC  $\times$  GC experiments with thermal modulation the entire flow of carrier gas (and sample) typically passes through all columns, which calls for a rather awkward compromise in selecting the same mass-flow rate for the relatively wide 1D column and the relatively narrow 2D column. This problem is greatly aggravated in GC  $\times$  GC  $\times$  GC, where a relatively very narrow 3D column is added. Regarding the instrument setup, the modulation interface that connects columns between separation dimensions is one of the most important features of any multidimensional chromatography system. Modulators in 3D-GC can be divided in three categories, viz. thermal modulators, valve-based modulators and flow modulators. A recent detailed review on modulators, covering thermal and valve-based modulators, including the principles of modulation, are discussed by Bahaghighat et al.<sup>41</sup>

The first reported GC  $\times$  GC  $\times$  GC system was described in 2000 by Ledford and Billesbach.<sup>33</sup> They used two staggered heated sweeper modulators to connect the three separation columns. The heated sweeper was popular during the first few years of GC  $\times$  GC in the 1990s, but it was soon replaced by cold-jet (cryogenic) modulations<sup>36</sup> and valve-based modulators. An advantage of the latter is that—in principle—the mass-flow rate can be different in different dimensions.<sup>42</sup> Current designs based on valve-based modulators in GC  $\times$  GC  $\times$  GC mostly used are 6-port diaphragm valves,<sup>17–19,35</sup> in which the effluent from the preceding column is collected in sample loops, before being flushed with a carrier gas to the following column. In early developments of GC  $\times$  GC  $\times$  GC with diaphragm-valve modulators, a flame-ionization detector (FID) was implemented for detection to demonstrate enhanced selectivity in GC  $\times$  GC  $\times$  GC and proof-of-principle separation of chemical compound classes. However, the diaphragm valves used had some drawbacks regarding the temperature which could not exceed 175 °C. Also, FID has limitations regarding the specificity of analyte detection and the possibilities for identification. In a later study by Watson et al. these drawbacks were overcome by replacing the FID with a time-of-flight mass spectrometer (ToF-MS) and implementing high-temperature diaphragm valves, which allowed increased operating temperatures and decreased sample splitting. The new design added mass-spectral information and led to higher peak capacities.<sup>35</sup>

Another unique valve-based modulator that has gained popularity over the years is the pulse flow modulator that was introduced by Cai et al. in 2004<sup>43</sup> and has been used mostly in the group of Synovec. The technique utilizes partial modulation by adding narrow pulses of carrier gas (down to 50 ms) to the regular gas flow in a Y-shaped connector. This allowed the creation of very narrow peaks superimposed on the largely unaffected one-dimensional chromatogram. Providing both 1D-GC and GC  $\times$  GC information in a single run. The effect of modulation development and techniques will be described in the following section.

As mentioned before a typical GC  $\times$  GC  $\times$  GC instrument comprises three capillary columns connected in-series using two modulators, with the final (3D) column interfaced with a detection system. However, some groups developed other interesting configurations. Chen et al. developed an ingenious 3D-GC system, which consisted of three sets of columns of different polarities, representing three dimensions of separation (1  $\times$  3  $\times$  6-channel 3D-GC configurations)<sup>34</sup> as shown in Figure 1. It allowed for independent control over each

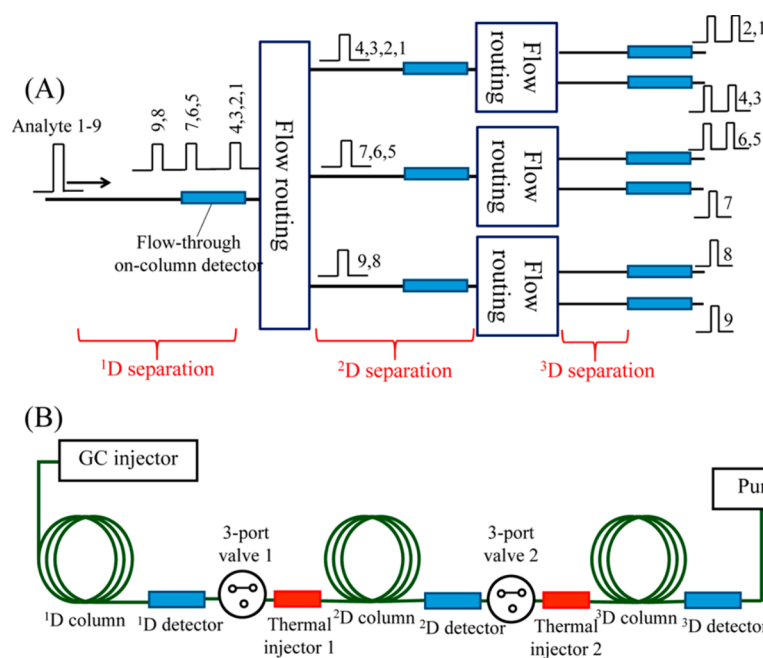


**Figure 1.** Schematic overview of a so-called “smart three-dimensional gas chromatograph”: (A) 3D-GC configuration with  $1 \times 3 \times 6$ -channels and (B) schematic configuration of  $1 \times 1 \times 1$ -channel 3D-GC setup. Reprinted with permission from 34. Copyright 2013 American Chemical Society.

dimension of separation. The 1D separation acted as a pre-separation stage, in which analytes were regrouped before entering the 2D-GC subsystem, which increased the time available for 2D and 3D separation and improved the overall performance of the system. The 1D and 2D columns were equipped with optical vapor detectors, followed by a flow-routing module consisting of a three-port valve and a thermal injector. The system may be attractive for multiple-heart-cut 3D-GC separations, if the interface between the columns maintains the integrity of the separation and the sample. For comprehensive  $GC \times GC \times GC$  separations, there may be a data-analysis challenge to merge the different data sets that represent parts of the sample. Moreover, the time gained to perform the different separations is not dramatic. Since a 2D separation should typically be 100 times faster than a 1D separation, it should still be some 30 times faster if three parallel 2D columns are installed and the six 3D columns should still operate 1700 times faster than the 1D column (instead of 10 000 times faster). In combination with the merging of data sets and the possible variations in conditions, the challenges are enormous.

Systems equipped with Dean-switch modulators have been successfully used in heart-cutting GC methods.<sup>36,38,39</sup> Sciarrone et al. presented the use of a 3D-preparative GC system consisting of three GC systems, equipped with Deans-switch devices, to couple the different columns. They showed it to be an effective tool for the isolation of a target compound at milligrams level from a complex sample matrix for further investigation through other analytical techniques.

**2.1.1. Physical Considerations.** Many additional parameters should be taken into account when setting up a 3D-GC instrument. For example, column temperature has a significant effect on retention, but also on selectivity, especially for polar phases and compounds. Some 3D-GC systems utilize a dual-oven setup,<sup>19,33,35,36,39</sup> in which the 1D column is placed in the main oven and the 3D column in a secondary oven. The 2D column may be positioned in the main oven with the 1D column

or in the secondary oven with a 3D column. Mommers and van der Wal<sup>31</sup> investigated how the overall selectivity could be tuned by varying the temperature offset of the secondary oven relative to the main system oven. A temperature program was used in a 3D-GC setup to resolve complex samples that featured a broad range of analyte retention and this was found to aid in the development of a high-throughput 3D-GC system that was fast without showing a significant loss in resolution.

## 2.2. Column Considerations

The stationary phases and column dimensions in a multi-dimensional system should be selected carefully. The choice of  $GC \times GC$  column sets has been discussed in many reviews.<sup>31,44,45</sup> However, for  $GC \times GC \times GC$ , the stationary-phase chemistry and the order of columns have not been fully investigated to achieve maximal orthogonality. Moreover, the column dimensions and operating conditions (temperature programs, flow rates) have not been optimized to attain the highest possible peak capacity. In this section, we highlight some important issues raised in the literature. The choice of the stationary-phase chemistries of the column-set depends on the sample characteristics and should be based on the expected types and strengths of the molecular interactions between the analytes and the stationary phase. The latter has been discussed in detail in a review by Mommers and van der Wal.<sup>31</sup> Ionic liquids—or liquid salts—are a relatively novel type of stationary-phases, which are commercially available and are claimed to offer several advantages. These include high thermal stability resulting in very low column bleed, a high polarity, and a broad range of applications. Siegler et al.<sup>18</sup> were the first to use a triflate ionic-liquid column as the 2D column in their  $GC \times GC \times GC$  setup, showing high selectivity for phosphonated compounds. They studied a diesel sample spiked with three different phosphonated compounds to demonstrate the separation power of their  $GC \times GC \times GC$  system. They found that a  $GC \times GC$  instrument with a suitable column combination was adequate to separate the matrix, but that all three dimension columns were needed to

separate the phosphonated compounds, while still providing useful information on the entire sample. Other interesting stationary-phase chemistries are needed to create a column with chiral selectivity. Wong et al.<sup>36</sup> described an automated online 3D-GC system that integrated several GC methods in one instrument to study on-column isomerization reactions. The enantioselective 1D column allowed the separation of diastereo- and enantiopure isomers, which were further separated using an ionic liquid 2D column. The pure isolated enantiomers were then selectively heart-cut, cryofocused, and subjected to a reactor column. After the reactor, these fractions were injected on the 3D column for achiral separations, which was said to allow for quantification of each *E* and *Z* isomer of each pair of enantiomers. Using different selectivities allowed the authors to isolate the region of interest from the sample matrix for online conversion, which resulted in the enrichment of enantiomers. The use of different columns with retention characteristics makes it important to also consider the order in which the different stationary phases are applied in a column set based on the expected analytes and their anticipated molecular interactions with the stationary-phases.<sup>31</sup> Many examples can be found in literature in which “non-polar  $\times$  medium-polar  $\times$  polar” column-sets are used for the analysis of mixtures of small molecules, allergens, or volatile and essential oils derived from natural products. Mostly, these samples concerned less polar analytes in polar matrices. By using a nonpolar 1D column, the separation is according to the boiling point. The following 2D and 3D columns, which exhibit polar interactions, will then provide separation according to polarity ranges yielding group-type information on both the sample and the matrices. It is recommended to use the least polar columns that provide sufficient retention, separation, and orthogonality. Highly polar columns are inferior in terms of robustness, and thermal stability and are prone to show more bleeding. Ionic liquid columns may suffer less from these disadvantages. However, as in GC  $\times$  GC, where polar  $\times$  nonpolar combinations exist as exceptions to the much more common nonpolar  $\times$  polar combinations. Several studies have been published in which the column order was the opposite from the conventional nonpolar  $\times$  medium polar  $\times$  polar<sup>18,19,35,38</sup> (see Table 2).

### 2.3. Peak Capacity

One motivation for the development of multidimensional separation systems, such as GC  $\times$  GC, is to obtain greater separation power (i.e., higher peak capacities), to obtain as much chemical information as possible on complex samples. The addition of a 2D column that shows different retention characteristics (e.g., a different polarity) allows for an enhanced selectivity, improved separation and a great increase in peak capacity. Any coeluting analytes in the first dimension may be resolved in the second dimension to approach more complete separations. The same motivators—separation power and selectivity—have spurred researchers to progress from GC  $\times$  GC to GC  $\times$  GC  $\times$  GC. The group of Synovec et al.<sup>17</sup> first reported a peak capacity for their GC  $\times$  GC  $\times$  GC-FID instrument. At that point, their GC  $\times$  GC  $\times$  GC setup yielded a peak capacity of 3500 during a total analysis time of 60 min (58 peaks/min). Improvements in the stationary phases, such as the use of ionic liquids have allowed them to enhance the peak production rate by about 3-fold to resolved peaks/min in a 20 min separation of diesel fuel.<sup>18</sup> However, their GC  $\times$  GC  $\times$  GC-instrument yielded a similar peak capacity compared

with the GC  $\times$  GC system. Under-sampling (i.e., too few modulations across a peak) and lack of instrument optimization were reported to affect the peak capacity. The instrument was improved by replacing the FID detector with ToF-MS and the face-mounted diaphragm valves of the modulator with a high-temperature diaphragm valve. This resulted in an average peak capacity of 7000 (140 peaks/min) for 10 representative analytes during a 50 min separation on the GC  $\times$  GC  $\times$  GC-ToF-MS instrument.<sup>35</sup> Yan et al.<sup>40</sup> created a GC<sub>NP</sub>–GC<sub>PEG</sub>  $\times$  GC<sub>IL</sub> system, where the subscripts indicate nonpolar (NP), poly(ethylene glycol) (PEG), and ionic liquid (IL) stationary phases. They obtained a peak capacity of about 5000 (40 peaks/min) for the analysis of agarwood oleoresin. This separation power was very similar to those achieved in state-of-the-art GC  $\times$  GC studies, in which the peak capacities ranged from 4000 to 7000. However, GC  $\times$  GC  $\times$  GC is expected to yield a gain in peak capacity in comparison to GC  $\times$  GC, although the gain is not expected to be quite as large as the 20- to the 30-fold gain obtained when progressing from 1D-GC to GC  $\times$  GC. In recent years, the group of Synovec has focused on improving the GC  $\times$  GC  $\times$  GC instruments. To increase the 3D peak capacities specifically concentrated on modulator technology, which is arguably the heart of comprehensive multidimensional GC systems. In 2018, they implemented a pulse-flow-valve modulator between the second and third dimensions, which provided ultrafast modulation pulses of 60 ms and allowed them to achieve an average peak capacity for a 115-component test mixture of about 10 000 across an 11 min separation window.<sup>20</sup> More recently, they achieved a peak capacity of 30 600 in 40 min (765 peaks/min) with the same 3D-system setup.<sup>37</sup> The authors focused on the relative phase ratios of the columns in the different separation dimensions to maximize the peak capacity. Using partial modulation using a pulse flow valve operated in a negative pulse mode to create extremely narrow, local analyte concentration pulses, the same group obtained 3D peaks with a peak width-at-base of 15 ms resulted in a GC  $\times$  GC  $\times$  GC peak capacity of about 35 000 in a 45 min separation.<sup>16</sup> The gain in peak capacities, thus, demonstrated during the past few years is extremely promising. Further gains in peak capacities can be expected as ongoing developments in GC  $\times$  GC  $\times$  GC instrumentation are made.

**2.3.1. Data-Analysis Algorithms.** Over many years, chemometric deconvolution techniques have been used in conjunction with set-ups that produce three-dimensional data. A leading such technique has been the Parallel Factor Analysis (PARAFAC) method, which is a natural expansion of principal-component analysis (PCA) for multivariate data.<sup>46</sup> A GC  $\times$  GC  $\times$  GC system produces multivariate data, which are compatible with PARAFAC methods. PARAFAC is suitable to analyze the 3D analyte signals and to resolve these from whatever overlap with any interfering components in all three separation dimensions. It provides deconvolution of analyte peaks for each separation dimension, which significantly increases the effective 3D-GC peak capacity.<sup>17</sup> Previously, PARAFAC was shown to provide benefits for dealing with overlapped ellipsoids when implemented in GC  $\times$  GC  $\times$  GC-FID systems.<sup>17,18</sup> Watson et al.<sup>17</sup> showed that the PARAFAC algorithm could mathematically resolve components that were not sufficiently separated chromatographically. For example, they were able to completely resolve heptane and 2-pentanol ellipsoids in their sample data, which showed no chromatographic resolution in any separation dimensions.



Since analytes at much lower chromatographic resolution can be mathematically separated, they concluded that PARAFAC allowed for an increase in the effective peak capacity of the instrument. Moreover, Watson et al. showed an approximately 10-fold increase in signal-to-noise ratio from the raw data to the deconvoluted data, because the PARAFAC algorithm removed a large portion of the noise as a factor separate from the analyte-signal factor. Later, Watson et al.<sup>19</sup> implemented the PARAFAC algorithm in their GC  $\times$  GC  $\times$  GC-TOFMS system, which added another dimension to the data. They applied it for targeted analyte discovery and deconvolution analysis cyclohexyl benzene, which occurs naturally in diesel fuels. The algorithm proved to resolve the cyclohexyl benzene signal from the coeluting peaks in the chemical background. Moreover, mass-spectral matching of the PARAFAC loadings to library spectra yielded high similarity values for 40 different analytes. However, the down-side of this technique was that the user needed sufficient prior knowledge on the target analyte. Ferreira et al.<sup>47</sup> have used PARAFAC for both qualitative and quantitative analyses using the GC  $\times$  GC  $\times$  GC-FID system for allergens in perfumes. They were able to resolve peaks of carvone and geraniol, which were coeluting in all three separation dimensions, but were successfully deconvoluted with the use of PARAFAC.

#### 2.4. Coupling to Various Chromatographic Approaches

Limitations in group-type separation for the analysis of mineral-oil samples with GC  $\times$  GC, based on the polarity and volatility of analytes, have pushed researchers to couple various other chromatographic approaches, such as liquid chromatography (LC) or supercritical-fluid chromatography (SFC) to GC  $\times$  GC. Characterization of complex oil and petrochemical samples has been a key application of GC  $\times$  GC from the beginning. Additional separation within a group, such as the separation between linear and cyclic alkanes is hard to accomplish. Since saturated cyclic hydrocarbons (naphthenes) are considered of great importance for the petrochemical industry, the need for the separation of these compounds is evident. It is possible to separate naphthenic compounds from acyclic alkanes using a stationary phase that exhibits phenylic interactions. However, Beens et al.<sup>48</sup> reported that the application of these types of stationary phases resulted in an overlap of naphthenes and aromatic compounds. By gaining resolution and selectivity between linear and cyclic alkanes, resolution and selectivity between cyclic alkanes and aromatics were reduced. GC  $\times$  GC fails to separate the naphthenes from the aromatics. Additional selectivity is required, besides volatility and polarity as sample dimensions. Other analytical methods, based on GC  $\times$  GC techniques hyphenated with liquid chromatography (LC) fractionation, have been considered as good alternatives for oil fractions, such as vacuum gas oils (VGOs) and essential oils. Table 3 shows a detailed overview of 3D separations based on LC or SFC techniques hyphenated with GC  $\times$  GC. The applications are categorized as off-line (F) and online (N) set-ups. As seen in Table 2, for comprehensive coupling of each dimension is denoted with "X" and heart-cutting methods are denoted with "-". Furthermore, we classified methods through the type of modulation used between the 1D and 2D columns (mode 1) and between the 2D and 3D columns (mode 2). The modulation types are abbreviated, as indicated in the table heading. For NPLC separations, we specified the retention

mechanism in Table 3, also this will be discussed later in the review.

Frysiner et al. examined the chemical composition of unresolved complex mixtures (UCM) of hydrocarbons in oil-contaminated marine sediments.<sup>49</sup> The UCM hydrocarbons were extracted and liquid-chromatographically separated on a silver-impregnated silica-gel column into four fractions, prior to GC  $\times$  GC analysis. Compared to the nonfractionated samples, this approach provided a better resolution and improved peak identification. However, a complete separation of classes was not achieved, since some hydrocarbon groups were distributed across more than one fraction. Edam et al.<sup>21</sup> used an amino-bonded silica HPLC column, for prefractionation based on the regulatory IP391 method. The many (104 for one sample) collected fractions were subsequently analyzed by GC  $\times$  GC. Group-type separation was achieved for both cycloalkanes and aromatics. The Edam method provided a separation of naphthenic classes, such as dinaphthenic and trinaphthenic alkanes, which would have overlapped with monoaromatic compounds in a GC  $\times$  GC separation. Figure 2A shows an LC-GC  $\times$  GC chromatogram of the saturated fraction, showing the naphthenic classes to be resolved according to the number of naphthenic rings. Unfortunately, this method was less suited for polycyclic aromatic hydrocarbons (PAHs) beyond diaromatics because of their late elution and associated band broadening, which causes a serious dilution. Also, the elution pattern of certain groups, such as alkenes, was not investigated in this method, due to their absence from common oil products. However, when characterizing oil-contaminated soils, processed oils with a high-alkene content may be encountered. Therefore, an LC-GC  $\times$  GC/FID method using a silver-loaded HPLC column as a prefractionation step before the GC  $\times$  GC analysis has been developed by Mao et al.<sup>23</sup> They used their method to separate oil hydrocarbons into alkane, cycloalkane, alkene, and (poly)-aromatic fraction, which could be further separated according to boiling point or equivalent carbon (EC) numbers, as shown in Figure 2B. The band-broadening and dilution problems observed when using silica or amino-bonded-silica columns were overcome using silver-based columns. The dilution was reduced, thanks to the narrow peaks obtained. Adding a prefractionation step significantly improved the group-type separation of oil hydrocarbons in comparison with the two-dimensional GC  $\times$  GC method. Also, improved quantitative results were obtained with the LC-GC  $\times$  GC method than with the direct GC  $\times$  GC analysis, thanks to the improved separation. In another study, this method was used to study the biodegradation and detailed monitoring of petroleum hydrocarbons in soil.<sup>22,23</sup>

GC  $\times$  GC has also been used to analyses heavy oil fractions, such as vacuum gas oils (VGOs). However, many coelutions occur owing to the very high number of compounds and the limited second-dimension selectivity at high temperatures, revealing significant drawbacks of the GC  $\times$  GC method. To resolve the coelution problem, Dutriez et al.<sup>53,54</sup> implemented an off-line LC separation step prior to GC  $\times$  GC analysis. LC column filled with silica and alumina was used to carry out a separation between saturated, aromatic, and more-polar (resin) compounds. By avoiding coelutions between saturates and monoaromatics and improving the GC  $\times$  GC conditions, an extensive characterization of poly and mononaphthenic compounds was achieved. Using high temperatures in the comprehensive two-dimensional gas-chromatography stages



**Table 3. Overview of Three-Dimensional Separations Based on Comprehensive Two-Dimensional Gas Chromatography with Normal-Phase Liquid-Chromatographic or Supercritical-Fluid Chromatographic Pre-fractionation (NPLC-GC × GC, SFC-GC × GC)<sup>a</sup>**

| application  | 1D type, dimensions $L$ (m) × i.d. ( $\mu\text{m}$ ), film thickness, $d_f$ ( $\mu\text{m}$ ) | mode 1 | 2D type, dimensions $L$ (m) × i.d. ( $\mu\text{m}$ ), film thickness, $d_f$ ( $\mu\text{m}$ )          | LC-based | mode 2                | 3D type, dimensions $L$ (m) × i.d. ( $\mu\text{m}$ ), film thickness, $d_f$ ( $\mu\text{m}$ )   | detection | total analysis time (min) | ref |
|--|---|--------|--|----------|-----------------------|---|-----------|---------------------------|-----|
| hydrocarbons in sediment sample                    | silica gel/silver-impregnated silica gel  | F – M  | nonpolar (poly dimethyl siloxane, 9.5 m × 100 $\mu\text{m}$ i.d., $d_f$ 0.5 $\mu\text{m}$ )            | N ×      | TM                    | medium-polar (14% cyanopropylphenyl polysiloxane, 0.75 m × 100 $\mu\text{m}$ i.d., $d_f$ 0.14 $\mu\text{m}$ )   | FID       | 270 (2D-GC)               | 49  |
| hydrocarbons (diesel fuel)                         | amino-bonded silica   | F – M  | nonpolar (dimethylpolysiloxane, 10 m × 250 $\mu\text{m}$ i.d., $d_f$ 0.25 $\mu\text{m}$ )              | N ×      | CM                    | medium-polar (50% polysilphenylene-siloxane, 2 m × 100 $\mu\text{m}$ i.d., $d_f$ 0.10 $\mu\text{m}$ )   | FID       | 130                       | 21  |
| hydrocarbons (middle distillates)                  | silica/gamma-alumina  | F – M  | nonpolar (dimethylpolysiloxane, 15 m × 200 $\mu\text{m}$ i.d., $d_f$ 0.5 $\mu\text{m}$ )               | N ×      | CM (CO <sub>2</sub> ) | medium-polar 50% phenyl-polysilphenylene-siloxane or 20% permethylated $\beta$ -cyclo dextrin, 1 m × 100 $\mu\text{m}$ i.d., $d_f$ 0.1 $\mu\text{m}$ )                    | FID       | –                         | 50  |
| hydrocarbons (soil samples)                        | silver-modified column  | F – M  | nonpolar (dimethylpolysiloxane, 30 m × 320 $\mu\text{m}$ i.d., $d_f$ 0.25 $\mu\text{m}$ )              | N ×      | CM (CO <sub>2</sub> ) | medium-polar (50% phenyl polysilphenylene-siloxane, 2.5 m × 100 $\mu\text{m}$ i.d., $d_f$ 0.1 $\mu\text{m}$ )   | FID       | 140                       | 24  |
| diesel sample                                      | amino-based column  | F – M  | nonpolar (poly dimethyl siloxane, 30 m × 250 $\mu\text{m}$ i.d., $d_f$ 0.25 $\mu\text{m}$ )            | N ×      | CM                    | polar (polyethylene glycol, 1.5 m × 100 $\mu\text{m}$ i.d., $d_f$ 0.1 $\mu\text{m}$ )   | MS        | 95                        | 51  |
| hydrocarbons (soil sample)                         | silver-modified column  | F – M  | nonpolar (dimethylpolysiloxane, 30 m × 320 $\mu\text{m}$ i.d., $d_f$ 0.25 $\mu\text{m}$ )              | N ×      | PV                    | medium-polar (50% phenyl polysilphenylene-siloxane, 2.0 m × 100 $\mu\text{m}$ i.d., $d_f$ 0.1 $\mu\text{m}$ )   | FID       | 160                       | 23  |
| hydrocarbons (soil sample)                         | silver-modified column  | F – M  | nonpolar (5% diphenyl dimethyl polysiloxane, 15 m × 250 $\mu\text{m}$ i.d., $d_f$ 0.25 $\mu\text{m}$ ) | N ×      | PV                    | medium-polar (50% phenyl polysilphenylene-siloxane and a 14% cyanopropylphenyl 86% dimethyl polysiloxane, 15 m × 250 $\mu\text{m}$ i.d., $d_f$ 0.25 $\mu\text{m}$ )       | FID       | –                         | 22  |
| aromatic hydrocarbons (MOSH/MOAH)                  | lichrospher SI column   | F – M  | nonpolar (dimethylpolysiloxane, 20 m × 250 $\mu\text{m}$ i.d., $d_f$ 0.12 $\mu\text{m}$ )              | N ×      | CM                    | polar (50% phenyl methyl polysiloxane, 1.5 m × 150 $\mu\text{m}$ i.d., $d_f$ 0.075 $\mu\text{m}$ )  | FID       | 60                        | 52  |
| vacuum gas oils                                    | silica/alumina  | F – M  | nonpolar (dimethylpolysiloxane, 10 m × 320 $\mu\text{m}$ i.d., $d_f$ 0.10 $\mu\text{m}$ )              | N ×      | CM (N <sub>2</sub> )  | medium-polar (50% phenyl polysilphenylene-siloxane, 0.5 m × 100 $\mu\text{m}$ i.d., $d_f$ 0.10 $\mu\text{m}$ )  | TOF-MS    | –                         | 53  |
| vacuum gas oils                                    | silica-based  | F – M  | medium-polar (dimethylpolysiloxane, 10 m × 320 $\mu\text{m}$ i.d., $d_f$ 0.10 $\mu\text{m}$ )          | N ×      | PV                    | medium-polar (50% phenyl polysilphenylene-siloxane, 0.5 m × 100 $\mu\text{m}$ i.d., $d_f$ 0.10 $\mu\text{m}$ )  | TOF-MS    | 80                        | 54  |
| hydrocarbons (essential oils)                      | silica-based  | F – M  | nonpolar (silyphenylene polymer, 30 m × 250 $\mu\text{m}$ i.d., $d_f$ 0.25 $\mu\text{m}$ )             | N ×      | PV                    | polar (polyethylene glycol, 1.0 m × 100 $\mu\text{m}$ i.d., $d_f$ 0.10 $\mu\text{m}$ )  | MS        | 65                        | 55  |
| coal tar samples (S-containing aromatic compounds) | silica-based  | N – P  | nonpolar (silyphenylene polymer, 30 m × 250 $\mu\text{m}$ i.d., $d_f$ 0.25 $\mu\text{m}$ )             | N ×      | PV                    | polar (polyethylene glycol, 1.0 m × 100 $\mu\text{m}$ i.d., $d_f$ 0.10 $\mu\text{m}$ )  | MS        | 91                        | 56  |
| hydrocarbon mixtures, diesel samples               | silver-based column   | N – CM | nonpolar (polydimethylsiloxane, 15 m × 200 $\mu\text{m}$ i.d., $d_f$ 1.0 $\mu\text{m}$ )               | N ×      | CM (CO <sub>2</sub> ) | medium-polar (50% phenyl-polysilphenylene-siloxane, 4.0 m × 100 $\mu\text{m}$ i.d., $d_f$ 0.1 $\mu\text{m}$ and 1.6 m × 100 $\mu\text{m}$ i.d., $d_f$ 0.1 $\mu\text{m}$ ) | FID       | 220                       | 57  |
| heavy petroleum fractions                          | cyanopropyl-silica (1), silver-modified silica (2), aminopropyl-silica (3)                    | N – P  | nonpolar (dimethylpolysiloxane, 10 m × 320 $\mu\text{m}$ i.d., $d_f$ 0.1 $\mu\text{m}$ )               | N ×      | CM (CO <sub>2</sub> ) | medium-polar (50% phenyl-polysilphenylene-siloxane, 0.8 m × 100 $\mu\text{m}$ i.d., $d_f$ 0.1 $\mu\text{m}$ )   | FID       | –                         | 27  |
| vacuum gas oils                                    | cyanopropyl-silica (1), silver-modified silica (2), aminopropyl-silica (3)                    | N × P  | nonpolar (dimethylpolysiloxane, 10 m × 320 $\mu\text{m}$ i.d., $d_f$ 0.1 $\mu\text{m}$ )               | N ×      | CM (CO <sub>2</sub> ) | medium-polar (50% phenyl-polysilphenylene-siloxane, 0.8 m × 100 $\mu\text{m}$ i.d., $d_f$ 0.1 $\mu\text{m}$ )   | FID       | –                         | 25  |

Table 3. continued

| application                              | 1D type, dimensions $L$ (m) $\times$ i.d. ( $\mu\text{m}$ ), film thickness, $d_f$ ( $\mu\text{m}$ ) | mode 1 | 2D type, dimensions $L$ (m) $\times$ i.d. ( $\mu\text{m}$ ), film thickness, $d_f$ ( $\mu\text{m}$ ) | mode 2        | 3D type, dimensions $L$ (m) $\times$ i.d. ( $\mu\text{m}$ ), film thickness, $d_f$ ( $\mu\text{m}$ )   | detection | total analysis time (min) | ref |  |
|--|--|--------|--|---------------|--|-----------|---------------------------|-----|--|
|  |  |        | SFC-based  |               |  |           |                           |     |  |
| analysis of Fischer–Tropsch oil products | PVA-column (1), silica column (2), silver-based column (3)   | N – P  | polar (polyethylene glycol, 60 m $\times$ 2.50 $\mu\text{m}$ i.d., $d_f$ 0.25 $\mu\text{m}$ )        | N $\times$ CM | $d_f$ 0.1 $\mu\text{m}$ and 1.45 m $\times$ 100 $\mu\text{m}$ i.d., $d_f$ 0.1 $\mu\text{m}$<br>nonpolar (diphenyldimethyl polysiloxane, 2 m $\times$ 100 $\mu\text{m}$ i.d., $d_f$ 0.1 $\mu\text{m}$ ) | TOF-MS    | 135                       | 58  |  |

<sup>a</sup>The mode columns indicate off-line (F) or on-line (N) coupling, hyphenation (–) or comprehensive coupling ( $\times$ ), passive modulation (M), manual modulation (M), and the type of modulator for GC  $\times$  GC, namely, thermal modulation (TM), cryogenic modulation (CM), and a three/six-port valves (PV).

(LC-HT-GC  $\times$  GC) made it possible to obtain near-molecular details on saturated and aromatic compounds in heavy oil fractions. This approach was applied to various VGOs and a wide range of other samples. It is noteworthy that all the above-mentioned LC-GC  $\times$  GC studies were carried out in an off-line manner. Collecting multiple fractions off-line induces risks of analyte loss and contamination or degradation of sample components during the collection and reconcentration steps. This would suggest that an online prefractionation step would be desirable. However, such methods have rarely been reported. Recently, Zoccali et al. developed a method based on an online combination of normal-phase liquid chromatography (NPLC) hyphenated to comprehensive GC  $\times$  GC with triple-quadrupole (QqQ) MS detection (i.e., NPLC-GC  $\times$  GC-QqQ-MS) for the analysis of coal tar.<sup>56</sup> The NPLC stage separated three classes of coal-tar compounds, namely, nonaromatic hydrocarbons, unsaturated compounds (with and without sulfur in the molecules), and oxygenated compounds. These three fractions were transferred via a syringe-based interface mounted on the autosampler of the GC  $\times$  GC instrument, which had been described in detail in an earlier study.<sup>59</sup> Zoccali et al. claimed that their system could be used in a variety of configurations, depending on specific analytical requirements. However, coupling an LC dimension online to a GC  $\times$  GC system to construct an online three-dimensional system is not trivial. An important factor to consider concerns the large volumes resulting from the HPLC separation, which are unsuitable for direct transfer to GC. Special interfaces are needed to remove the HPLC solvent. Another drawback is that the solvents used in the LC method resulted in dilution of the sample and possible contamination with impurities present in the solvent.

Supercritical-fluid chromatography (SFC) utilizes carbon dioxide ( $\text{CO}_2$ ) as the main component of the mobile phase. This appears to be more compatible with a gas-phase separation than LC. Therefore, the hyphenation of SFC to GC  $\times$  GC is easier to realize as demonstrated by several groups, as shown in Table 3. The same groups that developed LC-GC  $\times$  GC instruments also introduced the hyphenation of SFC with the GC  $\times$  GC system for similar applications of oil regarding analysis,<sup>25,27,57</sup> creating new prospects for online hyphenated 3D techniques. Potgieter et al. developed an online hyphenated SFC-GC  $\times$  GC system to comprehensively characterize the chemical classes, such as (linear and cyclic) saturates, (linear and cyclic) unsaturates, oxygenates, and aromatics fractions, present in light-oil samples obtained from a high-temperature Fischer–Tropsch (HT-FT) process.<sup>58</sup> The SFC setup (Figure 3) consisted of an oven equipped with two six-port two-position switching valves. Switching these allowed group-type separations by forward-flushing and back-flushing of the columns. The SFC columns-set used consisted of a silica column coated with poly(vinyl alcohol) (PVA) that was used to retain the oxygenates, a Petrosil silica column used to separate the aromatic from unsaturates, and a PetroAG silver-loaded cation-exchange column used to retain all the unsaturates. The SFC effluent was directed through an external six-port, two-position switching valve to either the FID detector of the SFC instrument or to the GC  $\times$  GC instrument. Once the retention ranges for each group were determined using the FID detector, the external valve could be switched at appropriate times to transfer the SFC fractions to the GC  $\times$  GC setup. The column-set for the latter consisted of a polar first-dimension column and a nonpolar second-

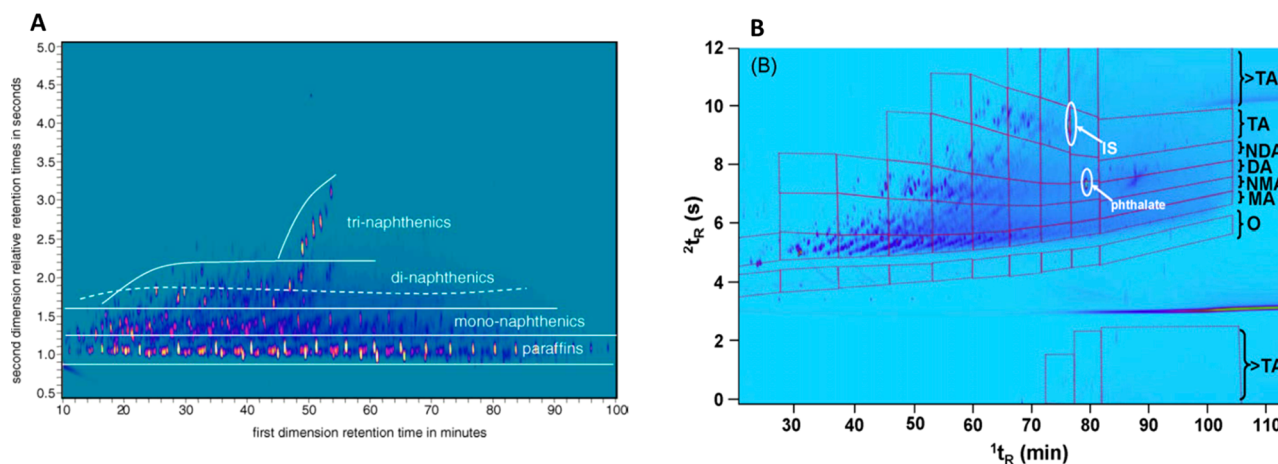


**Figure 2.** LC-GC  $\times$  GC chromatograms of oil samples. (A) LC-GC  $\times$  GC chromatogram of saturated fractions with structured elution within naphthenic classes. (B) LC-GC  $\times$  GC chromatogram of unsaturated fractions (O = alkenes, MA = monoaromatics, NMA = naphthenic monoaromatics, DA = diaromatics, NDA = naphthenic diaromatics, TA = triaromatics). Windows defined by every two equivalent carbon (EC) numbers in the first dimension. Panel A: Reprinted with permission from ref 21. Copyright 2005 Elsevier. Panel B: Reprinted with permission from ref 23. Copyright 2009 Elsevier.

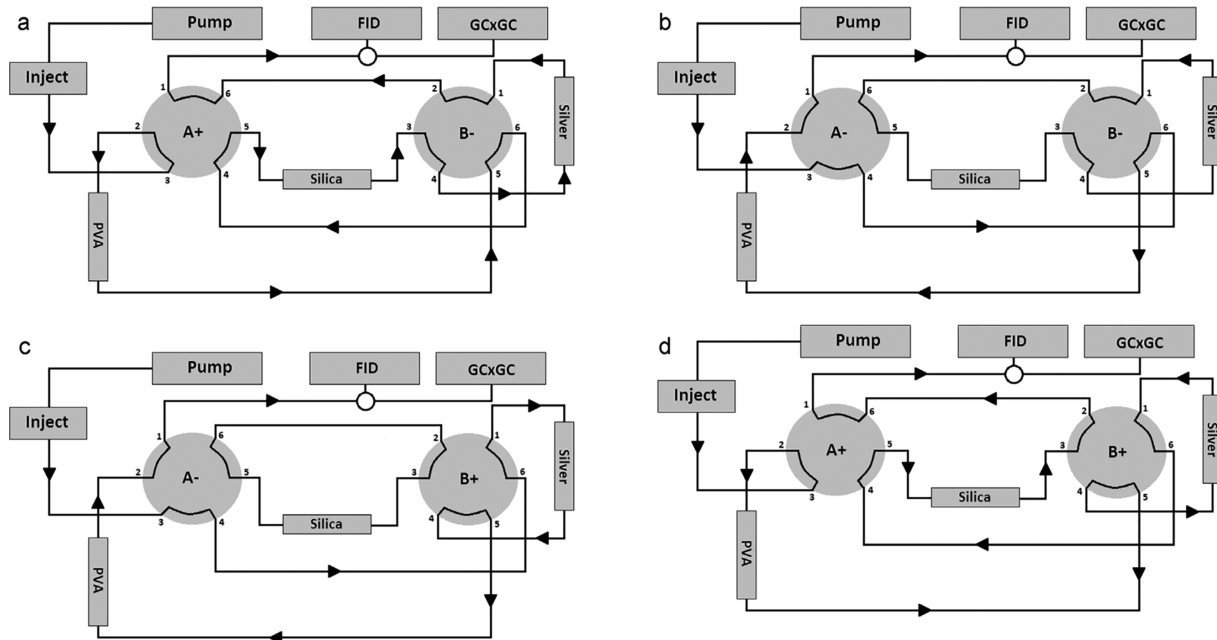


**Figure 3.** SFC column configurations for the elution of four fractions from light-oil samples. (A) Valve A operated in forward-flush mode, oxygenates fractions are retained on PVA column. (B) Valve A switched to negative position, PVA column operated in back-flush mode, while silica and silver column are in stop-flow mode (saturates). (C) Aromatics retained on silica column, valve A switched off, valve B switched on, to backflush the PVA and silver column for unsaturated fraction. (D) Both valves switched on for the forward-flush mode to elute aromatics. Reprinted with permission from ref 58. Copyright 2013 American Chemical Society.

dimension column, connected with the aid of a cryogenic modulator. The choice of a polar  $\times$  nonpolar column-set in contrast to the conventional nonpolar  $\times$  polar combination was based on previous work by the same group, in which the advantages of the polar  $\times$  nonpolar combinations for the analysis of oil products was discussed (see also section 2.2). In regions where HPLC mobile phases interfered with the GC  $\times$  GC analysis, the SFC-GC  $\times$  GC systems was free of interferences as can be seen in Figure 4. It can also be seen that similar contour plots are obtained for the saturated and unsaturated hydrocarbons are observed from the LC-GC  $\times$  GC and SFC-GC  $\times$  GC combinations. A similar attempt to realize three-dimensional SFC  $\times$  GC  $\times$  GC was made by

Dutriez et al.<sup>27</sup> This shows that SFC was just effective as the separation obtained using HPLC. In general, this 3D-instrument opens up a new prospect for the implementation of a fully online 3D-separation within the field of gas-phase dimensions with three orthogonal retention mechanism.

### 3. THREE-DIMENSIONAL-LIQUID CHROMATOGRAPHY

Comprehensive two-dimensional liquid chromatography (LC  $\times$  LC) was first described by F. Erni and R.W. Frei<sup>60</sup> and has emerged during the last two decades as a strong candidate for separating complex samples that require more separation power that can be provided by 1D-LC. It is among the most

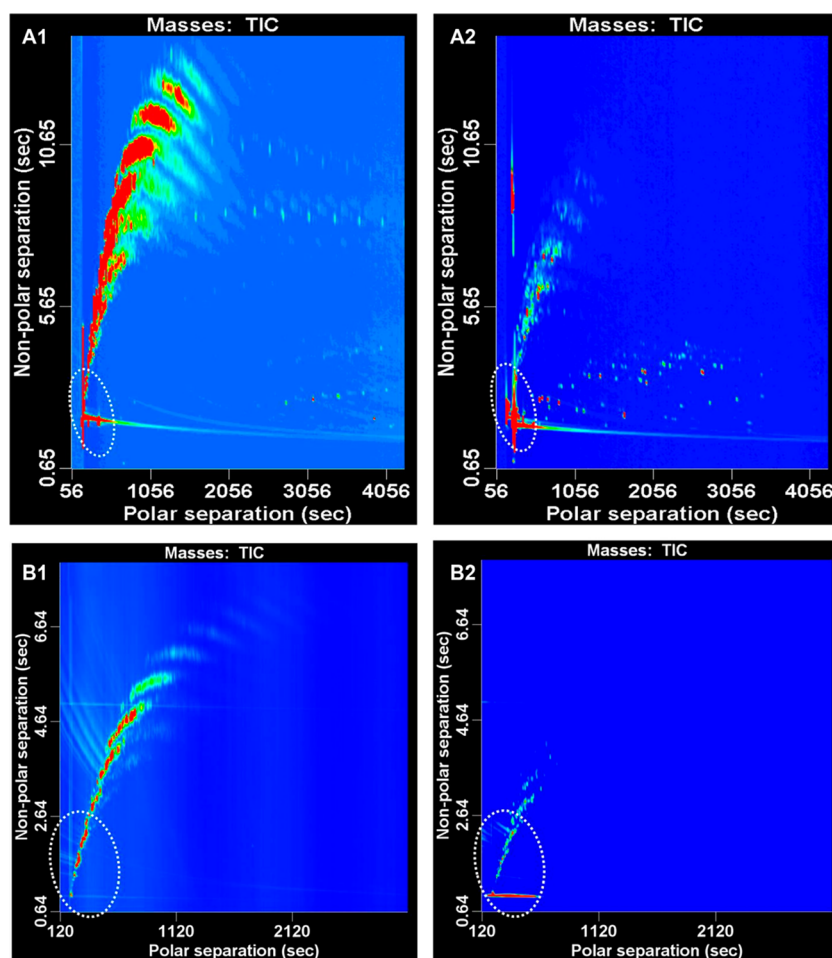


**Figure 4.** Comparison between the contour plots obtained from the HPLC GC  $\times$  GC–TOF-MS analysis of the (A1) saturate and (A2) unsaturate fractions and the SFC–GC  $\times$  GC–TOF-MS analysis of the (B1) saturate and (B2) unsaturate fractions of the same kerosene sample. (The circle indicates the area of concern where HPLC mobile phase elutes.) Reprinted with permission from ref 58. Copyright 2013 American Chemical Society.

powerful methods in many fields, such as polymer analysis, food analysis, environmental science, and most notably, in life science, including the field of proteomics. Usually, LC  $\times$  LC is performed in a “temporal” column-based format, ( $^t$ LC  $\times$   $^t$ LC). The sample is first separated in the 1D column, the effluent of which is divided into many fractions by a modulator. These fractions are then sequentially transferred to the 2D column for further separation. Many different retention mechanisms can be combined and LC  $\times$  LC can be coupled with various detectors for online characterization. Although LC  $\times$  LC methods are now well established and quite powerful, exhaustive separations of very complex samples are still challenging. This has motivated researchers to investigate the potential benefits of adding a third dimension (3D) LC column to an LC  $\times$  LC system, creating column-based LC  $\times$  LC  $\times$  LC as an alternative separation method. In comprehensive 3D-LC (LC  $\times$  LC  $\times$  LC) the entire 1D and 2D effluents must be transferred to the next dimension separation. This implies that a full second-dimension run should be completed during each modulation of the 1D effluent, so that the 2D separation should be very much faster than the 1D separation, and that the  $^3$ D separation should be even much faster than the 2D separation to realize a complete LC  $\times$  LC  $\times$  LC separation online in real-time. Physical parameters, such as column dimensions (internal diameter,

length), particle sizes, and flow rates must therefore be finely tuned to realize optimal LC  $\times$  LC  $\times$  LC separations. Because the 2D and, especially, the 3D separation has to be repeated many times during each analysis, columns packed with very small particles for ultrafast analysis must also be very robust and resistant to very high pressures, fast gradients and very high linear velocities, while providing sufficient efficiency to contribute significantly to the overall peak capacity of the system. Currently, sub-2- $\mu$ m particles are commonly used with ultrahigh pressure LC (UHPLC) systems. Such systems also cause minimal extra-column band broadening and exhibit very short dwell times. Vivó Truyols showed that smaller particles generally allow higher peak capacities to be achieved, rendering them well-suited for fast separations in the second and or third dimensions of multidimensional LC set-ups.<sup>61</sup> This conclusion is also readily apparent from the kinetic-plot concept, propagated by Desmet’s group<sup>62</sup>

At the early stages of developing 3D-LC, several systems were developed by the modification of the MudPIT 2D-LC approach to bottom-up proteomics (i.e., ion-exchange chromatography directly coupled with reversed-phase liquid chromatography for separating peptides<sup>63</sup> or offline 3D-LC systems. Recently, an elaborate review was published specifically on the topic of 3D separations for bottom-up proteomics, in which existing offline, and online 3D-LC



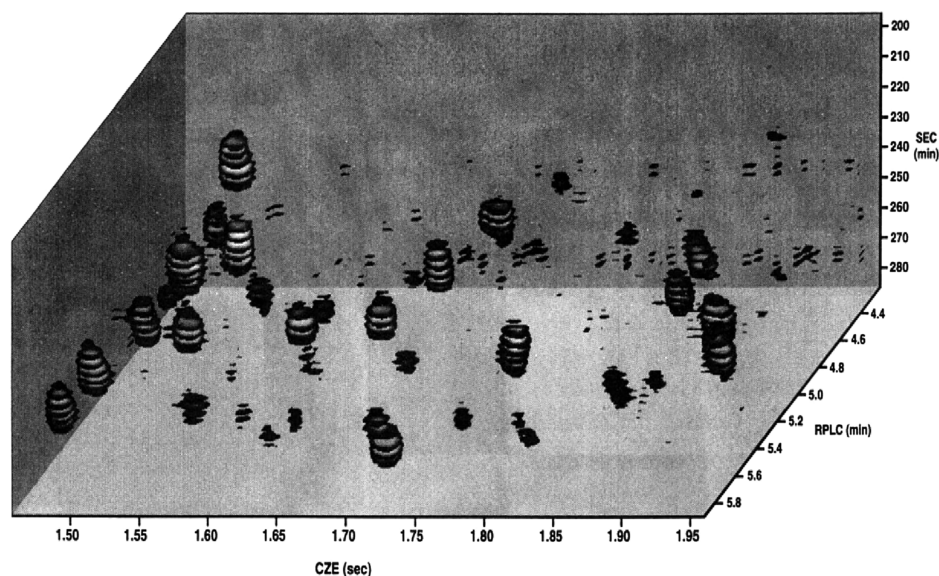


**Figure 5.** Three-dimensional representation of the data obtained from the three-dimensional separation of a peptide mixture, featuring 1D size-exclusion chromatography (SEC) plotted in the vertical direction, 2D reversed-phase liquid chromatography (RPLC; front to back), and 3D capillary zone electrophoresis (CZE, horizontal axis). Sizes of the disks indicate band intensity. Reprinted with permission from 12. Copyright 1995 American Chemical Society.

**Table 4. Overview of Time-Based LC<sup>3</sup> Platforms<sup>a</sup>**

| application                              | 1D  | mode 1 | 2D                                | mode 2 | 3D               | detection | ref |
|--|---|--------|-----------------------------------|--------|------------------|-----------|-----|
| organic compounds in wastewater          | RPLC (mixed-mode RPLC/weak cation exchange phase) | N – P  | RPLC (carbon-clad zirconia phase) | N – P  | RPLC (C18)       | UV        | 66  |
| peptides                                 | RPLC (pH 10, C18)                                 | N × P  | SAX (pH 10)                       | N × P  | RPLC (pH 3, C18) | MS        | 67  |
| THI analysis in caramel colors class III | RPLC (C18)  | N – S  | IEX                               | N – S  | RPLC (PGC)       | UV        | 68  |
| soybean extract                          | HILIC   | N × S  | RPLC (fluorophenyl)               | N × S  | RPLC (C18)       | ToF-MS    | 69  |
| amino acids (enantiomers)                | RPLC  | N – P  | WAX                               | N – P  | chiral           | FLD       | 70  |

<sup>a</sup>The couplings are N = online, × = comprehensive, – = heart-cut. The modulation types are P = passive, S = active stationary-phase assisted modulation (SPAM), QTof-MS = quadrupole time of flight mass spectrometer, and FLD = fluorescence detector.

platforms and combinations of both approaches in this field were summarized.<sup>28</sup> In the present Review, all existing online column-based 3D-LC methods for various applications will be discussed. Two-dimensional column-based (time-based) liquid chromatography (<sup>1</sup>LC × <sup>1</sup>LC) has verifiably produced much greater separation powers in much shorter analysis times than 1D-LC. However, an alternative approach to gain higher peak capacities is to conduct spatial two- and three-dimensional systems (<sup>2</sup>LC × <sup>2</sup>LC and <sup>3</sup>LC × <sup>3</sup>LC × <sup>3</sup>LC), which—in principle—may offer much higher separation power and short analysis time. Various approaches of spatial separation are described in this section. The reader is also referred to a recent review on the spatial based separations.<sup>64</sup>

To our knowledge, the first elaborate and powerful liquid-phase comprehensive three-dimensional separation method was described by Moore and Jorgenson<sup>12</sup> for the separation of hen-ovalbumin-derived peptides (see Figure 5). They coupled size-exclusion chromatography (SEC) and reversed-phase liquid chromatography (RPLC) in the first and second dimensions, respectively, and implemented capillary zone electrophoresis (CZE) in the third dimension. In conventional time-based gradient-elution 1D-LC, the peak capacity (<sup>1</sup>*n*<sub>c</sub>) can be approximated by eq 1, which can be rewritten as

$${}^1n_c \approx \frac{t_G}{t_0} \frac{\sqrt{L}}{4 \cdot R_s \cdot (1 + k_e) \cdot \sqrt{H}} + 1 \quad (5)$$

where *t*<sub>G</sub> is the duration of the gradient, *t*<sub>0</sub> the column hold-up time, *R*<sub>s</sub> is the desired resolution, *k*<sub>e</sub> the retention factor at the moment of the elution, *L* the column length, and *H* the (average) plate height. In a time-based 3D-LC system, the total peak capacity (<sup>3</sup>*n*<sub>c</sub>) can be approximated as the product of the peak capacities of each dimension. Unfortunately, Moore and Jorgenson achieved modest peak capacities in each dimension, namely, 5 for 1D SEC, 23 for 2D RPLC, and 24 for 3D CZE, resulting in a total peak capacity of about 2800. The authors encountered several challenges, such as high sample dilution during the three separation methods, which necessitated large sample injection volumes to achieve reasonable detection limits. The fractions obtained after the SEC separation (using methanol as mobile phase) had to be diluted with water prior to injection on the RPLC column. Moreover, the temperature needed rigorous control in all three dimensions, to avoid retention time drift caused by changes in temperature during the analysis. Another challenge faced was the presentation of the data and, in 1995, the need for a faster computer able to acquire data sufficiently fast and control the instrument so as to achieve more accurate timing. The overall comprehensive SEC

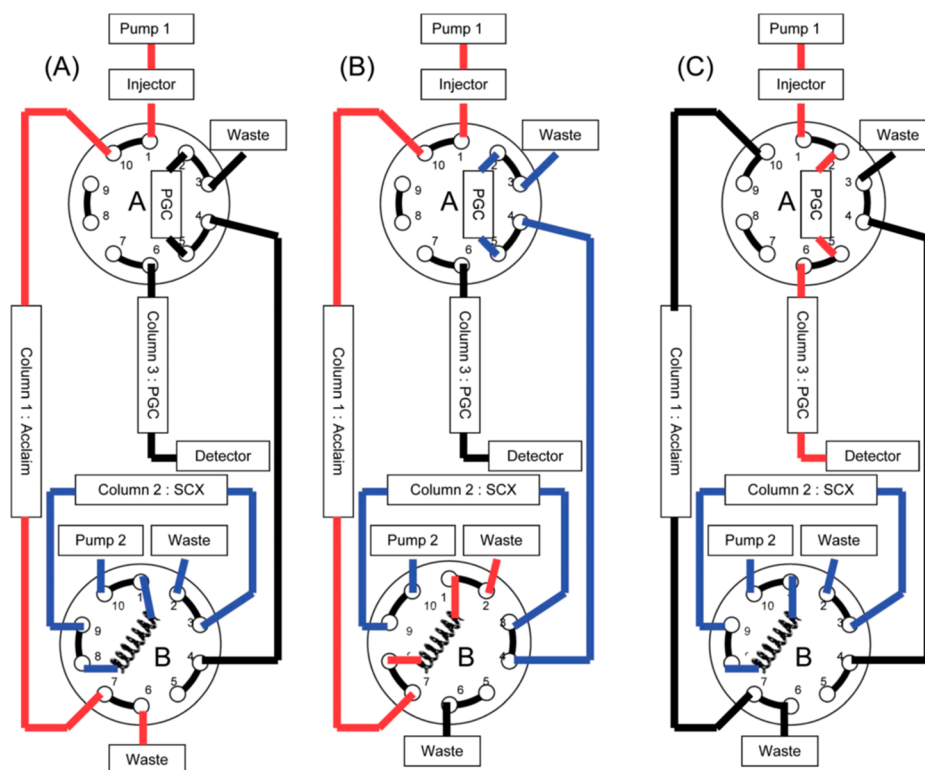


**Figure 6.** Experimental device for heart-cutting three-dimensional liquid chromatography: (A) separation on column 1 and column 2, (B) heart-cut at the outlet of column 1 and column 2, and (C) separation on column 3. Reprinted with permission from ref 68. Copyright 2016 American Chemical Society.

× RPLC × CZE separation required about 5 h analysis time, almost entirely due to the 1D SEC separation (280 min). The 2D RPLC separation took about 6 min and the 3D CZE separation about 6 s (see Figure 5). Despite the impressive results obtained in this pioneering work, few serious attempts were reported at tackling a full liquid-phase 3D-separation until about 15 years later.

Since then the implementation of online 3D-LC systems has covered a wide range of applications (see Table 4) and various combinations of retention mechanisms have been employed in such setups. In this Review, we focus on 3D-LC based system without electro-driven dimensions, although some researchers have used electro-driven separations in combination with LC-based techniques.<sup>65</sup> Chen et al. developed a three-dimensional SCX-RPLC-CZE platform (where SCX indicates strong cation exchange) for the analysis of a mouse-brain-proteome digest. With this method, an estimated peak capacity of about 7000 was achieved. However, other references do not mention the number of peak capacity; therefore, it is not included in this table.

The first selective heart-cutting 3D-LC method developed for targeted analysis was described by Simpkins et al.<sup>66</sup> The method was applied for the analysis of four different organic target compounds in aqueous samples using three functionally different reversed-phase HPLC columns. The choice of columns was based on the Hydrophobic Subtraction Model (HSM) for reversed-phase selectivity. The model indicates whether a pair of columns show sufficient differences in retention based on a specified set of solutes.<sup>71</sup> The authors achieved excellent separation of the target compound from the matrices, with relatively minor modifications to the separation conditions. Furthermore, a quantitative comparison of the 3D-

LC method with conventional (LC-MS/MS) methodology for trace analysis revealed no statistically significant difference between the concentrations of the target compound when a standard-addition method was used. Although the method showed promise, it was only suitable for a limited set of analytes with well-defined chemical structures. The group of Wang et al. developed an online LC<sup>3</sup> system for untargeted analysis of a complex soybean-extract sample by coupling a pre-separation column with comprehensive LC × LC using a stop-flow interface.<sup>69</sup> This latter interface was selected to overcome the challenges associated with long analysis time. The soybean extract served as a proof-of-principle to demonstrate the usefulness of the LC<sup>3</sup> system. This complex sample contained many classes of compounds, including nonpolar nonpolar lipids, weakly polar compounds, polar glycosylated compounds, flavonoids, oligosaccharides, etc. Pre-separation on the 1D amide column, divided the soybean extract into two fractions according to analyte polarities. Nonpolar and weakly polar analytes were collected in the first fraction and polar compounds in the second fraction. The fractions were captured on a trap column before being transferred to the 2D fluorophenyl and fractions from the 2D effluent were transferred to the 3D (C18) RPLC column, which finally was coupled to an MS detector. The LC<sup>3</sup> method established allowed identification of a number of important flavonoids within a total analysis time of less than 1 h. A total of 83 flavonoids were characterized, including many difficult-to-identify flavonoid isomers and low-abundance components. In total, some 30% more flavonoids were identified than had been found with a two-dimensional LC × LC method.

Another interesting 3D-LC setup was developed by Moreton et al. for the analysis of tetrahydrobutyl imidazole

(THI), a minor unwanted byproduct in class III caramel colors.<sup>68</sup> The heart-cutting 3D-LC system was based on the coupling of RPLC (C18), SCX, and RPLC (porous graphitic carbon, PGC) as 1D, 2D, and 3D stages, respectively (see Figure 6)

A single heart-cut of the 1D separation was stored in a 1 mL sample loop for a duration of 60 s, which was placed between the 1D column and a 10-port two-position valve. After switching the valve, the mixture trapped in the sample loop was subjected to the 2D separation and directed to the second 10-port two-position switching valve, which was integrated with a 10 mm × 4.0 mm i.d. PGC trap column, demonstrating the stationary-phase-assisted modulation (SPAM) technique.<sup>8</sup> Finally, after switching the second valve, the analytes focused on the trap column were eluted into the 3D column for the final separation. The total analysis time was 45 min. The mobile phases consisted of methanol/water (10/90 v/v) for the 1D system, 10 mmol/L ammonium formate adjusted to pH 2.5 with formic acid for the 2D system, and an ACN/water gradient with a final composition of 10/90 v/v for the 3D system. The authors took advantage of the hydrophobicity of the molecule both in the 1D and 3D separations, which might limit the orthogonality of the three dimensions. However, the separation of THI in a complex matrix was successfully achieved using the three separation mechanisms. The authors opted to maintain the same internal diameter for the columns of all dimension columns while varying the particle sizes. This may not concur with theoretical approaches to 2D-LC.<sup>9</sup> Conventional (passive) modulation, in which the effluent of one column is transferred unaltered to the next dimension. Active modulation techniques, such as SPAM or active-solvent modulation (ASM)<sup>8</sup> are aimed to focus the analyte band in a smaller volume, so that the diameter of the next column may be equal to or smaller than that of the previous one.

The single-heart-cut 3D-LC system proposed by Moretton et al. is far less constrained in terms of physical parameters than an online comprehensive LC<sup>3</sup> system would be. The main constraint for a single heart-cut 3D-LC system is that the volume of the sample loop needs to be sufficiently large to store the entire heart-cut effluent. The system contributions to band broadening need to be minimized. This, and the need to obtain sufficient sensitivity, may require active-modulation techniques, such as SPAM or ASM to be applied. In case trapping columns are used, their capacity and the conditions that allow rapid release of the analytes need to be considered as well.

The performance of the Moretton et al. 3D-LC method was evaluated in terms of precision and accuracy in a concentration range varying between 5 and 50 mg/kg of THI. When compared the heart-cut 3D-LC method for analysis of THI in caramel color class III to two 2D-LC methods for the same purpose, the 3D-LC system was found to be superior in terms of bias, precision, and accuracy. The heart-cut 3D-LC system was demonstrated to be advantageous for the analysis of a target compound in a very complex sample. However, the performance of such a system depends on the types of columns (stationary phases) and mobile phases that provide sufficient selectivity and orthogonality, (active) modulations, column dimensions and operating conditions, etc. The long analysis time remains an issue. This may potentially be addressed by introducing spatial two- and three-dimensional systems.

#### 4. SPATIAL 3D SEPARATION

Two-dimensional column-based (time-based) liquid chromatography (<sup>t</sup>LC × <sup>t</sup>LC) has verifiably produced much greater separation powers in much shorter analysis times than 1D-LC. However, even the peak capacities of 5000–10 000 that are readily achieved by <sup>t</sup>LC × <sup>t</sup>LC do not suffice for a number of applications. Limited progress has been made in the development and application of comprehensive three-dimensional LC, as discussed above. An alternative approach is to conduct spatial two- and three-dimensional systems (<sup>s</sup>LC × <sup>s</sup>LC and <sup>s</sup>LC × <sup>s</sup>LC × <sup>s</sup>LC), which—in principle—may offer much higher separation power and short analysis time.<sup>5</sup> To perform a spatial separation a body with two or more unified sets of separation parts needs to be constructed. Wouters et al. designed a spatial 3D-LC device where the three separation dimensions were fitted within a reasonably small area, namely, a microchip.<sup>72</sup> Another potential design for spatial 3D-LC was proposed by Adampoulou et al.<sup>73</sup> The analytes are first separated in a 1D channel, such that all analytes are positioned somewhere within the separation body. After developing the separation in the 1D channel, the analytes are transferred from the 1D channel in a perpendicular direction to the 2D region through the aid of a 2D flow-distributor. After developing the next separation in the 2D region, the analytes will then be further transferred to the 3D region using a 3D flow-distributor located on the top of the 2D region as shown in Figure 7.

The main advantage of this format in comparison with column-based LC<sup>3</sup> (<sup>t</sup>LC × <sup>t</sup>LC × <sup>t</sup>LC) is that first all second-dimension separations and then all three-dimensional separa-

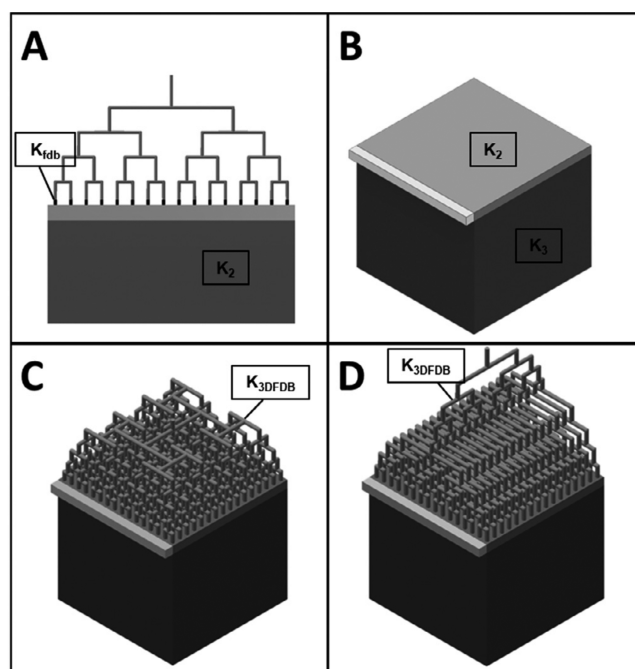


**Figure 7.** Simplified geometry for spatial LC<sup>3</sup> with the incorporation of a 3D flow distributor. (A) Spatial 2D-LC geometry, (B) simplified geometry for spatial 3D-LC, where  $K_2$  represents the 2D bed permeability and  $K_3$  represents the 3D cube permeability (C) a simplified geometry for spatial 3D-LC with the addition of a type-A flow distributor, (D) as (C), except with 3D-flow distributor,  $K_{3DFDB}$  is the permeability of the imposed porous zone in the top part of the 3D-flow distributor. Reprinted with permission from ref 73. Copyright 2020 American Chemical Society.



tions are performed simultaneously rather than sequentially. Therefore, the time required for an  ${}^x\text{LC} \times {}^x\text{LC}$  separation is the sum of the 1D and 2D analysis times. This is unlike  ${}^1\text{LC} \times {}^1\text{LC}$ , where the total analysis time is the product of the 2D run time and the number of fractions taken, which are often longer than the analysis time of the first dimension separation when performed on its own. Performing all separations in parallel presents an even greater advantage in the third dimension. Moreover, spatial separations should theoretically outperform column-based separations in terms of peak capacity. Davydova et al. used a Pareto-optimization approach to calculate the potential performance of various types of systems in terms of peak capacity. It was concluded that  ${}^x\text{LC} \times {}^x\text{LC} \times {}^x\text{LC}$  may reach peak capacities in the order of one million in a reasonable time and at very modest pressures.<sup>5</sup> To develop such a 3D separation body a number of challenges must be overcome. According to Guiochon et al., the three major problems that should be solved are (i) the packing of a homogeneous stationary phase in the different separation regions to ensure orthogonal retention mechanisms, (ii) the flow control and confinement, and (iii) the detection of the separated components of the sample.<sup>11</sup> During the past decade, several aspects of these challenges have been investigated, including chip fabrication,<sup>74</sup> design of flow-distributors,<sup>73,77</sup> and creation of stationary phase in different formats.<sup>78,79</sup> Computational fluid dynamics (CFD) has been a key tool in many of these studies. It offers a means to simulate liquid flow and mass transfer in a specific geometry. CFD is a reliable and powerful method to study the optimal conditions before experimental testing of a device. CFD has been used for studying the flow confinement and mass transfer in  ${}^x\text{LC} \times {}^x\text{LC}$  and  ${}^x\text{LC} \times {}^x\text{LC} \times {}^x\text{LC}$  designs.<sup>73</sup> Adamopoulou et al. investigated the possibility to employ permeability differences to guide the flow and reduce analyte loss within different compartments in  ${}^x\text{LC} \times {}^x\text{LC}$  and  ${}^x\text{LC} \times {}^x\text{LC} \times {}^x\text{LC}$  devices. In several studies, the synergy between CFD and prototype manufacturing was exploited to create optimal conditions prior to practical testing of microfluidic devices for spatial separation.

A novel way to create separation devices may be developed through the use of 3D-printing technology. During a relatively short time, 3D-printing technology has greatly advanced, and it has been adapted to a broad range of materials (e.g., thermoplastics, metals). These developments could not stay unnoticed in the field of chromatography.<sup>80</sup> Titanium is a strong material with high thermal conductivity and suitable surface chemistry to fabricate monolithic material within the housing. The strength was exploited in printed devices described by Passamonti et al.<sup>79</sup>, who demonstrated a method to create thermally initiated polymeric monolithic stationary phases within discrete regions of 3D-printed titanium devices. Monolithic stationary phases have gained a great deal of attention for incorporation in microfluidic devices. Passamonti et al.<sup>79</sup> were able to fabricate monoliths using several different approaches. One of these was based on recirculating jackets, which could be used for localized heating and cooling. This approach resembles a recirculation based on the freeze–thaw valve method.<sup>81</sup> Nawada et al. have used the latter method as a means for flow control in 3D-printed fluidic devices for spatial LC.<sup>82</sup> These studies have contributed to progress in spatial 3D-LC and the knowledge gained in these studies should contribute to the realization of successful spatial separation devices in the near future.

## 5. CONCLUSIONS

The need for further gains in peak capacities and enhanced chemical selectivity to separate very complex samples has motivated researchers to explore online 3D-separations. Interesting configurations have been developed in which three different separation dimensions are coupled online. Major progress has been made in modulation technology for GC, which has made efficient  $\text{GC} \times \text{GC} \times \text{GC}$  separations possible. Notably, the group of Synovec has used partial modulation through a pulse-flow valve, to achieve peak capacities of about 35 000—the highest values reported so far. Developments in  $\text{GC} \times \text{GC} \times \text{GC}$  instrumentation and column sets are still ongoing and there is still room for improvement, guided by a better understanding of the factors that govern 3D peak capacity. Coupling  $\text{GC} \times \text{GC}$  to another chromatographic separation, such as SFC, has created new prospects for integrated online 3D set-ups for much-improved (group type) separations. The development of online 3D-LC systems with various combinations of retention mechanisms has been reported for a wide range of applications. Successful implementations of column-based (time-based) 3D-LC concern almost exclusively heart-cut systems. The requirements for successful time-based comprehensive  $\text{LC} \times \text{LC} \times \text{LC}$  have drastic consequences, such as extreme demands on the speed and robustness of second-dimension and, especially, third-dimension separations, very long overall analysis times, major constraints on modulators and significant data-handling and data-analysis challenges. Therefore, researchers have begun to explore alternative formats, such as spatial two- and three-dimensional systems, which potentially offer much greater peak capacities, along with short analysis time. However, some key challenges must be addressed to make spatial 3D-LC live up to its great promise for the separation of complex samples

## AUTHOR INFORMATION

### Corresponding Author

**Noor Abdulhussain** – Van't Hoff Institute for Molecular Sciences and The Centre for Analytical Sciences Amsterdam (CASA), University of Amsterdam, 1098 XH Amsterdam, The Netherlands; Email: [n.abdulhussain@uva.nl](mailto:n.abdulhussain@uva.nl)

### Authors

**Suhas Nawada** – Van't Hoff Institute for Molecular Sciences and The Centre for Analytical Sciences Amsterdam (CASA), University of Amsterdam, 1098 XH Amsterdam, The Netherlands

**Peter Schoenmakers** – Van't Hoff Institute for Molecular Sciences and The Centre for Analytical Sciences Amsterdam (CASA), University of Amsterdam, 1098 XH Amsterdam, The Netherlands; [orcid.org/0000-0002-9167-7716](https://orcid.org/0000-0002-9167-7716)

Complete contact information is available at:  
<https://pubs.acs.org/10.1021/acs.chemrev.0c01244>

### Notes

The authors declare no competing financial interest.

### Biographies

Noor Abdulhussain obtained her M.Sc. degree in 2017 from the University of Amsterdam and the Vrije Universiteit Amsterdam. She is now a PhD student in the ERC STAMP (Separation Technology for A Million Peaks) project at the University of Amsterdam. Abdulhussain has published on integrated analysis of nanoparticles



and the constituting macromolecules by LC  $\times$  LC. She recently was decorated with the best poster award at HPLC2019 (Milan, Italy) and was invited to give a lecture at the Emerging Separations Technologies symposium (Chromatographic Society, London, UK). In 2019, LC-GC identified her as one of the Rising Stars in Chromatography. While her current work mainly focuses on functionality assessments of 3D-printed devices for application to multidimensional separations, Abdulhussain remains involved in studying fundamental separation mechanisms including hydrodynamic chromatography and size-exclusion chromatography.

Suhas Nawada is a postdoctoral researcher in the STAMP project (Separation Technology for a Million Peaks) at the University of Amsterdam's Van't Hoff Institute of Molecular Sciences (HIMS). He obtained his Masters in Chemical Engineering from the University of Sheffield (UK). Then, he moved to the University of Christchurch, Canterbury, NZ, where he performed his PhD research on the development of 3D printed stationary phases under the supervision of Prof. Conan Fee and Dr. Simone Dimartino. His work involves proof-of-concept 3D printed chromatographic stationary phases and micro and milli-fluidic 3D-printed platforms for multidimensional separations. He is the inventor of hybrid stereolithography.

Peter Schoenmakers is a professor of Analytical Chemistry at the University of Amsterdam. He investigates analytical separations, focussing on multidimensional liquid chromatography. He studied in Delft, The Netherlands (with Professor Leo de Galan) and in Boston, MA (with Professor Barry Karger). Thereafter, he worked for Philips in Eindhoven (The Netherlands) and for Shell in Amsterdam and in Houston, TX. He was awarded the AJP Martin Medal in 2011, the John Knox medal in 2014, the Csaba Horváth Award and the CASSS Award in 2015, the Fritz-Pregl Medal in 2018 and the Dal Nogare Award in 2019. In 2016, he obtained an Advanced Grant for Excellent Research from the European Research Council.

## ACKNOWLEDGMENTS

The STAMP project is funded under Horizon 2020-Excellent Science-European Research Council (ERC), Project 694151. The sole responsibility of this publication lies with the authors. The European Union is not responsible for any use that may be made of the information contained therein. Ahmet Taskale is acknowledged for his assistance in this Review.

## REFERENCES

- (1) Davis, J. M.; Giddings, J. C. Statistical Theory of Component Overlap in Multicomponent Chromatograms. *Anal. Chem.* **1983**, *55*, 418–424.
- (2) Vivó-Truyols, G.; van der Wal, S.; Schoenmakers, P. J. J. Comprehensive Study on the Optimization of Online Two-Dimensional Liquid Chromatographic Systems Considering Losses in Theoretical Peak Capacity in First- and Second-Dimensions: A Pareto-Optimality Approach. *Anal. Chem.* **2010**, *82*, 8525–8536.
- (3) Horie, K.; Kimura, H.; Ikegami, T.; Iwatsuka, A.; Saad, N.; Fiehn, O.; Tanaka, N. Calculating Optimal Modulation Periods to Maximize the Peak Capacity in Two-Dimensional HPLC. *Anal. Chem.* **2007**, *79*, 3764.
- (4) Schoenmakers, P. J.; Vivó-Truyols, G.; Decrop, W. M. C. A Protocol for Designing Comprehensive Two-Dimensional Liquid Chromatography Separation Systems. *J. Chromatogr. A* **2006**, *1120*, 282–290.
- (5) Davydova, E.; Schoenmakers, P. J.; Vivó-Truyols, G. Study on the Performance of Different Types of Three-Dimensional Chromatographic Systems. *J. Chromatogr. A* **2013**, *1271*, 137–143.
- (6) Stoll, D. R.; Carr, P. W. Two-Dimensional Liquid Chromatography: A State of the Art Tutorial. *Anal. Chem.* **2017**, *89*, 519–531.

- (7) Giddings, J. C. Sample Dimensionality: A Predictor of Order-Disorder in Component Peak Distribution in Multidimensional Separation. *J. Chromatogr. A* **1995**, *703*, 3–15.

- (8) Pirok, B. W. J.; Stoll, D. R.; Schoenmakers, P. J. Recent Developments in Two-Dimensional Liquid Chromatography: Fundamental Improvements for Practical Applications. *Anal. Chem.* **2019**, *91*, 240–263.

- (9) Pirok, B. W. J.; Gargano, A. F. G.; Schoenmakers, P. J. Optimizing Separations in Online Comprehensive Two-Dimensional Liquid Chromatography. *J. Sep. Sci.* **2018**, *41*, 68–98.

- (10) Groeneveld, G.; Pirok, B. W. J.; Schoenmakers, P. J. Perspectives on the Future of Multi-Dimensional Platforms. *Faraday Discuss.* **2019**, *218*, 72–100.

- (11) Guiochon, G.; Marchetti, N.; Mriziq, K.; Shalliker, R. A. Implementations of Two-Dimensional Liquid Chromatography. *J. Chromatogr. A* **2008**, *1189*, 109–168.

- (12) Moore, A. W.; Jorgenson, J. W. Comprehensive Three-Dimensional Separation of Peptides Using Size Exclusion Chromatography/Reversed Phase Liquid Chromatography/Optically Gated Capillary Zone Electrophoresis. *Anal. Chem.* **1995**, *67*, 3456–3463.

- (13) Nolvachai, Y.; Kulsing, C.; Marriott, P. J. Multidimensional Gas Chromatography in Food Analysis. *TrAC, Trends Anal. Chem.* **2017**, *96*, 124–137.

- (14) Dymerski, T. Two-Dimensional Gas Chromatography Coupled With Mass Spectrometry in Food Analysis. *Crit. Rev. Anal. Chem.* **2018**, *48*, 252–278.

- (15) Adahchour, M.; Beens, J.; Vreuls, R. J. J.; Brinkman, U. A. T. Recent Developments in Comprehensive Two-Dimensional Gas Chromatography (GC  $\times$  GC). III. Applications for Petrochemicals and Organohalogenes. *TrAC, Trends Anal. Chem.* **2006**, *25*, 726–741.

- (16) Gough, D. V.; Song, D. H.; Schöneich, S.; Prebihalo, S. E.; Synovec, R. E. Development of Ultrafast Separations Using Negative Pulse Partial Modulation to Enable New Directions in Gas Chromatography. *Anal. Chem.* **2019**, *91*, 7328–7335.

- (17) Watson, N. E.; Siegler, W. C.; Hoggard, J. C.; Synovec, R. E. Comprehensive Three-Dimensional Gas Chromatography with Parallel Factor Analysis. *Anal. Chem.* **2007**, *79*, 8270–8280.

- (18) Siegler, W. C.; Crank, J. A.; Armstrong, D. W.; Synovec, R. E. Increasing Selectivity in Comprehensive Three-Dimensional Gas Chromatography via an Ionic Liquid Stationary Phase Column in One Dimension. *J. Chromatogr. A* **2010**, *1217*, 3144–3149.

- (19) Watson, N. E.; Prebihalo, S. E.; Synovec, R. E. Targeted Analyte Deconvolution and Identification by Four-Way Parallel Factor Analysis Using Three-Dimensional Gas Chromatography with Mass Spectrometry Data. *Anal. Chim. Acta* **2017**, *983*, 67–75.

- (20) Bahaghighat, H. D.; Freye, C. E.; Gough, D. V.; Sudol, P. E.; Synovec, R. E. Ultrafast Separations via Pulse Flow Valve Modulation to Enable High Peak Capacity Multidimensional Gas Chromatography. *J. Chromatogr. A* **2018**, *1573*, 115–124.

- (21) Edam, R.; Blomberg, J.; Janssen, H. G.; Schoenmakers, P. J. Comprehensive Multi-Dimensional Chromatographic Studies on the Separation of Saturated Hydrocarbon Ring Structures in Petrochemical Samples. *J. Chromatogr. A* **2005**, *1086*, 12–20.

- (22) Mao, D.; Lookman, R.; Van De Weghe, H.; Weltens, R.; Vanermen, G.; De Brucker, N.; Diels, L. Combining HPLC-GCXGC, GCXGC/ToF-MS, and Selected Ecotoxicity Assays for Detailed Monitoring of Petroleum Hydrocarbon Degradation in Soil and Leaching Water. *Environ. Sci. Technol.* **2009**, *43*, 7651–7657.

- (23) Mao, D.; Lookman, R.; Van De Weghe, H.; Van Look, D.; Vanermen, G.; De Brucker, N.; Diels, L. Detailed Analysis of Petroleum Hydrocarbon Attenuation in Biopiles by High-Performance Liquid Chromatography Followed by Comprehensive Two-Dimensional Gas Chromatography. *J. Chromatogr. A* **2009**, *1216*, 1524–1527.

- (24) Mao, D.; Van De Weghe, H.; Diels, L.; De Brucker, N.; Lookman, R.; Vanermen, G. High-Performance Liquid Chromatography Fractionation Using a Silver-Modified Column Followed by Two-Dimensional Comprehensive Gas Chromatography for Detailed

Group-Type Characterization of Oils and Oil Pollutions. *J. Chromatogr. A* **2008**, *1179*, 33–40.

(25) Dutriez, T.; Thiébaud, D.; Courtiade, M.; Dulot, H.; Bertoncini, F.; Hennion, M. C. Application to SFC-GC × GC to Heavy Petroleum Fractions Analysis. *Fuel* **2013**, *104*, 583–592.

(26) Omais, B.; Dutriez, T.; Courtiade, M.; Charon, N.; Ponthus, J.; Dulot, H.; Thiébaud, D. SFC-GC×GC to Analyse Matrices from Petroleum and Coal. *LC GC Eur.* **2011**, *24*, 352–365.

(27) Dutriez, T.; Thiébaud, D.; Courtiade, M.; Dulot, H.; Bertoncini, F.; Hennion, M. C. Supercritical Fluid Chromatography Hyphenated to Bidimensional Gas Chromatography in Comprehensive and Heart-Cutting Mode: Design of the Instrumentation. *J. Chromatogr. A* **2012**, *1255*, 153–162.

(28) Duong, V. A.; Park, J. M.; Lee, H. Review of Three-Dimensional Liquid Chromatography Platforms for Bottom-up Proteomics. *Int. J. Mol. Sci.* **2020**, *21*, 1524.

(29) Giddings, J. C. *Unified Separation Science*; John Wiley and Sons Inc.: New York, 1991.

(30) Liu, Z.; Phillips, J. B. Comprehensive Two-Dimensional Gas Chromatography Using on-Column Thermal Modulator Interface. *J. Chromatogr. Sci.* **1991**, *29*, 227–231.

(31) Mommers, J.; van der Wal, S. Column Selection and Optimization for Comprehensive Two-Dimensional Gas Chromatography: A Review. *Crit. Rev. Anal. Chem.* **2021**, *51*, 183–202.

(32) Chin, S. T.; Marriott, P. J. Multidimensional Gas Chromatography beyond Simple Volatiles Separation. *Chem. Commun.* **2014**, *50*, 8819–8833.

(33) Ledford, E. B.; Billesbach, C. A.; Zhu, Q. GC 3: Comprehensive Three-Dimensional Gas Chromatography. *J. High Resolut. Chromatogr.* **2000**, *23* (3), 205–207.

(34) Chen, D.; Seo, J. H.; Liu, J.; Kurabayashi, K.; Fan, X. Smart Three-Dimensional Gas Chromatography. *Anal. Chem.* **2013**, *85*, 6871.

(35) Watson, N. E.; Bahaghighat, H. D.; Cui, K.; Synovec, R. E. Comprehensive Three-Dimensional Gas Chromatography with Time-of-Flight Mass Spectrometry. *Anal. Chem.* **2017**, *89*, 1793–1800.

(36) Wong, Y. F.; Kulsing, C.; Marriott, P. J. Switchable Enantioselective Three- and Four-Dimensional Dynamic Gas Chromatography-Mass Spectrometry: Example Study of On-Column Molecular Interconversion. *Anal. Chem.* **2017**, *89*, 5620–5628.

(37) Gough, D. V.; Bahaghighat, H. D.; Synovec, R. E. Column Selection Approach to Achieve a High Peak Capacity in Comprehensive Three-Dimensional Gas Chromatography. *Talanta* **2019**, *195*, 822–829.

(38) Mitrevski, B.; Marriott, P. J. Novel Hybrid Comprehensive 2D - Multidimensional Gas Chromatography for Precise, High-Resolution Characterization of Multicomponent Samples. *Anal. Chem.* **2012**, *84*, 4837–4843.

(39) Sciarrone, D.; Pantò, S.; Rotondo, A.; Tedone, L.; Tranchida, P. Q.; Dugo, P.; Mondello, L. Rapid Collection and Identification of a Novel Component from *Clausena lansium* Skeels Leaves by Means of Three-Dimensional Preparative Gas Chromatography and Nuclear Magnetic Resonance/Infrared/Mass Spectrometric Analysis. *Anal. Chim. Acta* **2013**, *785*, 119–125.

(40) Yan, D. D.; Wong, Y. F.; Whittock, S. P.; Koutoulis, A.; Shellie, R. A.; Marriott, P. J. Sequential Hybrid Three-Dimensional Gas Chromatography with Accurate Mass Spectrometry: A Novel Tool for High-Resolution Characterization of Multicomponent Samples. *Anal. Chem.* **2018**, *90*, 5264–5271.

(41) Bahaghighat, H. D.; Freye, C. E.; Synovec, R. E. Recent Advances in Modulator Technology for Comprehensive Two Dimensional Gas Chromatography. *TrAC, Trends Anal. Chem.* **2019**, *113*, 379–391.

(42) Bruckner, C. A.; Prazen, B. J.; Synovec, R. E. Comprehensive Two-Dimensional High-Speed Gas Chromatography with Chemometric Analysis. *Anal. Chem.* **1998**, *70*, 2796–2804.

(43) Cai, H.; Stearns, S. D. Partial Modulation Method via Pulsed Flow Modulator for Comprehensive Two-Dimensional Gas Chromatography. *Anal. Chem.* **2004**, *76*, 6064–6076.

(44) Mostafa, A.; Edwards, M.; Górecki, T. Optimization Aspects of Comprehensive Two-Dimensional Gas Chromatography. *J. Chromatogr. A* **2012**, *1255*, 38–55.

(45) Seeley, J. V.; Seeley, S. K. Multidimensional Gas Chromatography: Fundamental Advances and New Applications. *Anal. Chem.* **2013**, *85*, 557–578.

(46) Bro, R. Review on Multiway Analysis in Chemistry - 2000–2005. *Crit. Rev. Anal. Chem.* **2006**, *36*, 279–293.

(47) Ferreira, V. H. C.; Hantao, L. W.; Poppi, R. J. Consumable-Free Comprehensive Three-Dimensional Gas Chromatography and PARAFAC for Determination of Allergens in Perfumes. *Chromatographia* **2020**, *83*, 581–592.

(48) Beens, J.; et al. Proper Tuning of Comprehensive Two-Dimensional Gas Chromatography (GC×GC) to Optimize the Separation of Complex Oil Fractions. *J. High Resolut. Chromatogr.* **2000**, *23* (3), 182–188.

(49) Frysinger, G. S.; Gaines, R. B.; Xu, L.; Reddy, C. M. Resolving the Unresolved Complex Mixture in Petroleum-Contaminated Sediments. *Environ. Sci. Technol.* **2003**, *37*, 1653–1662.

(50) Adam, F.; Bertoncini, F.; Thiébaud, D.; Esnault, S.; Espinat, D.; Hennion, M. C. Of Middle Distillates by LC - GC × GC. *J. Chromatogr. Sci.* **2007**, *45*, 643–649.

(51) Sciarrone, D.; Quinto Tranchida, P.; Costa, R.; Donato, P.; Ragonese, C.; Dugo, P.; Dugo, G.; Mondello, L. Offline LC-GC × GC in Combination with Rapid-Scanning Quadrupole Mass Spectrometry. *J. Sep. Sci.* **2008**, *31*, 3329–3336.

(52) Biedermann, M.; Grob, K. Comprehensive Two-Dimensional GC after HPLC Preseparation for the Characterization of Aromatic Hydrocarbons of Mineral Oil Origin in Contaminated Sunflower Oil. *J. Sep. Sci.* **2009**, *32*, 3726–3737.

(53) Dutriez, T.; Courtiade, M.; Thiébaud, D.; Dulot, H.; Bertoncini, F.; Hennion, M. C. Extended Characterization of a Vacuum Gas Oil by Offline LC-High-Temperature Comprehensive Two-Dimensional Gas Chromatography. *J. Sep. Sci.* **2010**, *33*, 1787–1796.

(54) Dutriez, T.; Courtiade, M.; Thiébaud, D.; Dulot, H.; Borrás, J.; Bertoncini, F.; Hennion, M. C. Advances in Quantitative Analysis of Heavy Petroleum Fractions by Liquid Chromatography-High-Temperature Comprehensive Two-Dimensional Gas Chromatography: Breakthrough for Conversion Processes. *Energy Fuels* **2010**, *24*, 4430–4438.

(55) Tranchida, P. Q.; Zoccali, M.; Bonaccorsi, I.; Dugo, P.; Mondello, L.; Dugo, G. The Off-Line Combination of High Performance Liquid Chromatography and Comprehensive Two-Dimensional Gas Chromatography-Mass Spectrometry: A Powerful Approach for Highly Detailed Essential Oil Analysis. *J. Chromatogr. A* **2013**, *1305*, 276–284.

(56) Zoccali, M.; Tranchida, P. Q.; Mondello, L. On-Line Combination of High Performance Liquid Chromatography with Comprehensive Two-Dimensional Gas Chromatography-Triple Quadrupole Mass Spectrometry: A Proof of Principle Study. *Anal. Chem.* **2015**, *87*, 1911–1918.

(57) Adam, F.; Thiébaud, D.; Bertoncini, F.; Courtiade, M.; Hennion, M. C. Supercritical Fluid Chromatography Hyphenated with Twin Comprehensive Two-Dimensional Gas Chromatography for Ultimate Analysis of Middle Distillates. *J. Chromatogr. A* **2010**, *1217*, 1386–1394.

(58) Potgieter, H.; van der Westhuizen, R.; Rohwer, E.; Malan, D. Hyphenation of Supercritical Fluid Chromatography and Two-Dimensional Gas Chromatography-Mass Spectrometry for Group Type Separations. *J. Chromatogr. A* **2013**, *1294*, 137–144.

(59) Purcaro, G.; Zoccali, M.; Tranchida, P. Q.; Barp, L.; Moret, S.; Conte, L.; Dugo, P.; Mondello, L. Comparison of Two Different Multidimensional Liquid-Gas Chromatography Interfaces for Determination of Mineral Oil Saturated Hydrocarbons in Foodstuffs. *Anal. Bioanal. Chem.* **2013**, *405*, 1077–1084.

(60) Erni, F.; Frei, R.W.; et al. *J. Chromatogr. A* **1978**, *149*, 561–569.

(61) Vivó-Truyols, G.; Van Der Wal, S.; Schoenmakers, P. J. Comprehensive Study on the Optimization of Online Two-Dimensional Liquid Chromatographic Systems Considering Losses in

Theoretical Peak Capacity in First- and Second-Dimensions: A Pareto-Optimality Approach. *Anal. Chem.* **2010**, *82*, 8525–8536.

(62) Broeckhoven, K.; Cabooter, D.; Eeltink, S.; Desmet, G. Kinetic Plot Based Comparison of the Efficiency and Peak Capacity of High-Performance Liquid Chromatography Columns: Theoretical Background and Selected Examples. *J. Chromatogr. A* **2012**, *1228*, 20–30.

(63) Washburn, M. P.; Wolters, D.; Yates, J. R. Large-Scale Analysis of the Yeast Proteome by Multidimensional Protein Identification Technology. *Nat. Biotechnol.* **2001**, *19*, 242–247.

(64) Themelis, T.; Amini, A.; De Vos, J.; Eeltink, S. Towards Spatial Comprehensive Three-Dimensional Liquid Chromatography: A Tutorial Review. *Anal. Chim. Acta* **2021**, *1148*, 238157.

(65) Chen, D.; Shen, X.; Sun, L. Strong Cation Exchange-Reversed Phase Liquid Chromatography-Capillary Zone Electrophoresis-Tandem Mass Spectrometry Platform with High Peak Capacity for Deep Bottom-up Proteomics. *Anal. Chim. Acta* **2018**, *1012*, 1–9.

(66) Simpkins, S. W.; Bedard, J. W.; Groskreutz, S. R.; Swenson, M. M.; Liskutin, T. E.; Stoll, D. R. Targeted Three-Dimensional Liquid Chromatography: A Versatile Tool for Quantitative Trace Analysis in Complex Matrices. *J. Chromatogr. A* **2010**, *1217*, 7648–7660.

(67) Zhou, F.; Sikorski, T. W.; Ficarro, S. B.; Webber, J. T.; Marto, J. A. Online Nanoflow Reversed Phase-Strong Anion Exchange-Reversed Phase Liquid Chromatography-Tandem Mass Spectrometry Platform for Efficient and in-Depth Proteome Sequence Analysis of Complex Organisms. *Anal. Chem.* **2011**, *83*, 6996–7005.

(68) Moretton, C.; Nigay, H. Application of Three-Dimensional Liquid Chromatography for Quantification of 2-Acetyl-4-(1,2,3,4-Tetrahydroxybutyl)Imidazole (THI) in Caramel Colours. *Anal. Methods* **2016**, *8*, 6573–6579.

(69) Wang, S.; Shi, X.; Xu, G. Online Three Dimensional Liquid Chromatography/Mass Spectrometry Method for the Separation of Complex Samples. *Anal. Chem.* **2017**, *89*, 1433–1438.

(70) Furusho, A.; Koga, R.; Akita, T.; Mita, M.; Kimura, T.; Hamase, K. Three-Dimensional High-Performance Liquid Chromatographic Determination of Asn, Ser, Ala, and Pro Enantiomers in the Plasma of Patients with Chronic Kidney Disease. *Anal. Chem.* **2019**, *91*, 11569–11575.

(71) Snyder, L. R.; Dolan, J. W.; Carr, P. W. A New Look at the Selectivity of RPC Columns. *Anal. Chem.* **2007**, *79*, 3254–3262.

(72) Wouters, B.; Davydova, E.; Wouters, S.; Vivo-Truyols, G.; Schoenmakers, P. J.; Eeltink, S. Towards Ultra-High Peak Capacities and Peak-Production Rates Using Spatial Three-Dimensional Liquid Chromatography. *Lab Chip* **2015**, *15*, 4415–4422.

(73) Adamopoulou, T.; Deridder, S.; Bos, T. S.; Nawada, S.; Desmet, G.; Schoenmakers, P. J. Optimizing Design and Employing Permeability Differences to Achieve Flow Confinement in Devices for Spatial Multidimensional Liquid Chromatography. *J. Chromatogr. A* **2020**, *1612*, 460665.

(74) Davydova, E.; Wouters, S.; Deridder, S.; Desmet, G.; Eeltink, S.; Schoenmakers, P. J. Design and Evaluation of Microfluidic Devices for Two-Dimensional Spatial Separations. *J. Chromatogr. A* **2016**, *1434*, 127–135.

(75) Bushey, M. M.; Jorgenson, J. W. Automated Instrumentation for Comprehensive Two-Dimensional High-Performance Liquid Chromatography/Capillary Zone Electrophoresis. *Anal. Chem.* **1990**, *62*, 978–984.

(76) Adam, F.; Vendevre, C.; Bertoncini, F.; Thiébaud, D.; Espinat, D.; Hennion, M. C. Comprehensive Two-Dimensional Gas Chromatography for Enhanced Analysis of Naphthas: New Column Combination Involving Permethylated Cyclodextrin in the Second Dimension. *J. Chromatogr. A* **2008**, *1178*, 171–177.

(77) Adamopoulou, T.; Deridder, S.; Desmet, G.; Schoenmakers, P. J. Two-Dimensional Insertable Separation Tool (TWIST) for Flow Confinement in Spatial Separations. *J. Chromatogr. A* **2018**, *1577*, 120–123.

(78) Abdulhussain, N.; Nawada, S.; Currivan, S.; Passamonti, M.; Schoenmakers, P. Fabrication of Polymer Monoliths within the Confines of Non-Transparent 3D-Printed Polymer Housings. *J. Chromatogr. A* **2020**, *1623*, 461159.

(79) Passamonti, M.; Bremer, I. L.; Nawada, S. H.; Currivan, S. A.; Gargano, A. F. G.; Schoenmakers, P. J. Confinement of Monolithic Stationary Phases in Targeted Regions of 3D-Printed Titanium Devices Using Thermal Polymerization. *Anal. Chem.* **2020**, *92*, 2589.

(80) Salmean, C.; Dimartino, S. 3D-Printed Stationary Phases with Ordered Morphology: State of the Art and Future Development in Liquid Chromatography. *Chromatographia* **2019**, *82*, 443–463.

(81) Gerhardt, G. C.; Bouvier, E. S. P. D. T. Fluid Flow Control Freeze/Thaw Valve for Narrow Bore Capillaries or Microfluidic Devices. US 6557575, 2003.

(82) Nawada, S. H.; Aalbers, T.; Schoenmakers, P. J. Freeze-Thaw Valves as a Flow Control Mechanism in Spatially Complex 3D-Printed Fluidic Devices. *Chem. Eng. Sci.* **2019**, *207*, 1040–1048.